Aalto University
School of Chemical
Engineering

Paulus Ilmanen

MODELING OF THIN FILM EVAPORATOR FOR IONIC LIQUID RECYCLING

Master´s Programme in Chemical, Biochemical and Materials Engineering

Major in Chemical Engineering

Master's thesis for the degree of Master of Science in Technology submitted for inspection, Espoo, 21 May, 2017.

Supervisor Professor Ville Alopaeus

Instructor Kaj Jakobsson

Waqar Ahmad

Aalto University
School of Chemical
Engineering

Aalto University, P.O. BOX 11000, 00076 AALTO
www.aalto.fi

Abstract of master's thesis

Author Paulus Ilmanen

Title of thesis Modeling of thin film evaporator for ionic liquid recycling

Degree Programme Master's Programme in Chemical, Biochemical and Materials Engineering

Major Chemical engineering

Thesis supervisor Professor Ville Alopaeus

Thesis advisor(s) / Thesis examiner(s) Kaj Jakobsson, Waqar Ahmad

Date 21.05.2017 **Number of pages** 54 **Language** English

Abstract

World demand for textiles is on the rise and there is a need for fiber source that does not require arable land. Ioncell-F is a novel method of producing fiber from pulp. It uses ionic liquid [DBNH][OAc] to dissolve cellulose. Ionic liquid is expensive so it has to be recycled to make the process economical. Ionic liquid is thermally unstable, therefore the recycling has to be done with moderate temperatures. One way to separate and recycle ionic liquid from water is thin film evaporation.

The purpose of this study was to model the evaporation of water from water/[DBNH][OAc] mixture in an agitated thin film evaporator in flowsheet simulator Aspen Plus. Accurate modeling of the evaporator is needed to design and optimize the recycling process. The study also studied the applicability of multiple-effect evaporation.

Various modeling approaches were studied to simulate the thin film evaporator and an Aspen Plus model was developed based on batch distillation theory. The performance of the model was compared to an earlier developed model based on flash drum model and experimental data. The batch model gave more accurate results than the often used flash model. The model did not include the hydrolysis product of the ionic liquid, implementation of which should be the focus in future works. A case study was conducted and the applicability of double-effect evaporation was tested with the model. A rapid boiling point elevation at low water concentrations made it harder to implement multiple-effect evaporation in recycling of the ionic liquid. It could be done with right pressure and temperature settings for most of the evaporation, with one additional evaporator to achieve desired water content. Multiple-effect evaporation proved useful in both achieving purer vapor and lowering the total required heating power.

Keywords Ionic liquid, thin film evaporator, [DBNH][OAc], Ioncell-F

Aalto-yliopisto
Kemian tekniikan
korkeakoulu

Aalto-yliopisto, PL 11000, 00076 AALTO
www.aalto.fi

Diplomityön tiivistelmä

Tekijä Paulus Ilmanen

Työn nimi Ohutfilmihaiduttimen mallintaminen ionisen nesteen kierrättämiseksi

Koulutusohjelma Master's Programme in Chemical, Biochemical and Materials Engineerin

Pääaine Chemical engineering

Työn valvoja Professori Ville Alopaeus

Työn ohjaaja(t)/Työn tarkastaja(t) Kaj Jakobsson, Waqar Ahmad

Päivämäärä 21.5.2017 **Sivumäärä** 54 **Kieli** Englanti

Tiivistelmä

Maailmanlaajuinen tekstiilin kysyntä on kasvussa, ja tekstiilin lähteeksi tarvitaan raaka-aineita, jotka eivät vie tilaa viljeltävältä maalta. Ioncell-F on uusi prosessi, joka voi tuottaa kuitua sellusta. Se käyttää ionista nestettä [DBNH][OAc] liuottaakseen selluloosan. Ioninen neste on kallista, joten se täytyy erottaa vedestä ja kierrättää, jotta prosessi on kannattava. Se kuitenkin myös hajoaa korkeissa lämpötiloissa, joten erotus täytyy tehdä matalissa lämpötiloissa. Yksi keino tähän on ohutfilmihaihdutin.

Tämän työn tarkoituksena oli mallintaa veden haihdutusta veden ja ionisen nesteen seoksesta ohutfilmihaihduttimessa Aspen-Plus ohjelmalla. Haihduttimen tarkka mallinnus on tärkeää kierrätysprosessin suunnittelemiseksi ja optimoinniksi. Työssä myös selvitettiin, olisiko monivaihelauhdutus mahdollista.

Erilaisia malllinnusvaihtoehtoja käsiteltiin ja panostislaukseen pohjautuva malli valittiin keskittymispohjaksi. Aspen Plus malli kehitettiin panostislausteorian pohjalta, ja sen tuloksia verrattiin aiemmin kehitettyyn flash-malliin sekä kokeellisiin tuloksiin. Panostislausmallin tulokset olivat lähempänä kokeellisia, kuin flash-malli. Kummastakin mallista kuitenkin puuttuu ionisen nesteen hydrolyysituote, mikä tuo epätarkkuutta mallinnukseen. Sen sisältäminen mallinnukseen tulisi olla seuraavien tutkimusten kohde. Panostislausmallille tehtiin tapaustutkimus ja monivaihelauhdutuksen sisällyttämisen mahdollisuutta haihdutusprosessiin arvioitiin. Kiehumispisteen kohoama vähäisissä vesipitoisuuksissa on nopeaa, mikä vaikeuttaa monivaihelauhdutuksen käyttämistä. Oikeilla paineilla ja lämpötiloilla se saatiin kuitenkin sisällytettyä, jos viimeisen haihduttimen lämmittämiseen käytettiin ulkoista energiaa. Monivaihelauhdutus säästi selvästi lämmitysenergiaa sekä auttoi kierrätystä jakamalla höyryn suureen virtaan erittäin puhdasta vesihöyryä ja pienempään virtaan, jossa lähes kaikki höyrystynyt ioninen neste oli.

Avainsanat Ioninen neste, ohutfilmihaihdutin, [DBNH][OAc], Ioncell-F

Preface

This master's thesis was done for the chemical engineering research group at Aalto University School of Chemical Engineering from October 2016 to May 2017. I would like to thank my supervisor Ville Alopaeus and my instructors Kaj Jakobsson and Waqar Ahmad for patience and advice. I am also grateful for fellow thesis worker Max Zrunek and the researchers who were always ready to discuss and provide information when I had challenges with my work. The ability to discuss about the ideas considering my thesis was very helpful. Special thanks to my family for supporting me at every step during my studies at the university.

Contents

Nomenclature

A	Surface area (m^2)
c_p	Specific heat capacity ($\mathrm{J/kgK}$)
D	Evaporator diameter (m)
$\dot{D}$	Distillate molar flow (mol/s)
F	Feed to the evaporator ($\mathrm{kg/s}$)
h_o	External heat transfer coefficient (W/m^2K)
h_p	Internal heat transfer coefficient (W/m^2K)
J	Mass flux ($\mathrm{kg/m^2s}$)
k_L	Liquid side mass transfer coefficient (m/s)
L	Evaporator length (m)
$\dot{L}$	Liquid molar flow (mol/s)
N	Rotational speed of the evaporator blades ($1/\mathrm{s}$)
N_b	Number of blades in the evaporator
Nu	Nusselt number
Pr	Prandtl number
Q	Heating power (W)
Re	Reynolds number
Re_f	Film Reynolds number
Re_N	Rotational Reynolds number
Sc	Schmidt number
U	Overall heat transfer coefficient (W/m^2K)

$\dot{V}$	Volumetric flow rate (m^3/s)
v	velocity (m/s)
ΔT_{ln}	Logarithmic mean temperature difference (K)
β_h	heat transfer enhancement factor
Γ	Steam mass flow per unit length (kg/ms)
δ_{wall}	Wall thickness (m)
λ	Thermal conductivity (W/mK)
μ	Dynamic viscosity (Pas)
ν	Kinematic viscosity (m^2/s)
ω	Mass fraction

Introduction

Cotton is a traditional source for producing textile fiber. The world population is expected to rise and thus also the demand for food and textiles. In the lack of arable land to grow the cotton, other methods for producing textiles have to be developed. One alternative source of textile fiber is cellulose from pulp. (Hämmerle 2011)

Various methods of producing fiber from cellulose have been developed, such as Lyocell and Viscose processes. Both these processes have certain disadvantages. N-methylmorpholine N-oxide (NMMO) used in Lyocell process as a solvent is unstable and requires high temperatures to dissolute cellulose. Fibers produced by Viscose process have worse quality than fibers produced by other methods. A new promising process in development is Ioncell-F. (Ostonen et al. 2016)

Ioncell-F uses ionic liquid 1,5-diazabicyclo[4.3.0]non-5-enium acetate ([DBNH][OAc]) to dissolve cellulose in order to create fibers. Pulp and ionic liquid are mixed in a kneader due to high viscosity of the mixture and the resulting spinning dope is filtered. The fibers are produced from the spinning dope with dry jet wet spinning method. Dope is extruded through multiple holes in spinneret through air gap into a water bath. The fibers are spun from the bath and the remaining ionic liquid has to be concentrated in order to recycle it back to the process. According to Parviainen et al. (2015) recycling of ionic liquid is necessary for industrial adaptation due to high prices of ionic liquids. Their study also concluded that the water content of recycled ionic liquid should be less than 4 w-% to avoid decomposition of [DBNH][OAc]. One option to concentrate ionic liquid is to use a thermal separation method. Since ionic liquids decompose in high temperatures and the separation requires moderate temperature and short residence time. Thin film evaporation meets those requirements.

Modeling of [DBNH][OAc]-water evaporation with thin film evaporator is challenging due to the lack of thermodynamic data of ionic liquids in simulation programs. There also is no readily available model of the thin film evaporator in Aspen Plus. Ahmad et al. (2016) studied the evaporation behavior of [DBNH][OAc] and VLE of [DBNH][OAc]-water mixture. With this data, they constructed simulation model based on flash model in Aspen Plus and compared the results to the experimental results. They concluded that single stage flash model is reasonably accurate

but more rigorous model is needed. Purpose of this study is to model the thin film evaporator in Aspen Plus to study different modeling approaches in detail and compare their behavior to already existing experimental data by Ahmad et al. (2016). Accurate modeling of thin film evaporator is necessary for design and optimization of the process and thus a detailed evaporator model has to be developed. This work focuses on the hydrodynamical behavior in a flowsheeting environment.

LITERATURE REWIEW

1. Ionic liquid

Ionic liquids are molten salts with melting point below 100 ℃ (Parviainen et al. 2015). In this work the purpose of ionic liquid in the process is to dissolve cellulose to produce textile fibers. This study focuses on the ionic liquid used in Ioncell-F process, [DBNH][OAc].

[DBNH][OAc] is produced from DNB (1,5-Diazabicyclo[4.3.0]non-5-ene) and HOAc (acetic acid). Ostonen et al. (2016) give [DBNH][OAc] a melting point of 48 ℃. With the presence of water, DBN may undergo hydrolysis reaction to 1-(3-aminopropyl)-2-pyrrolidone (APP) which can form 3-(aminopropyl)-2-pyrrolidonium acetate ([APPH](OAc]) with acetic acid. This can further decompose into 1-(3-acetamidopropyl)-2-pyrrolidone (APPAc). These reactions are presented in figure 1. The hydrolysis step is a reversible reaction but further decomposition is irreversible (Parviainen et al. 2015). For this reason [DBNH][OAc] shoud not be exposed to high temperatures to avoid decomposition.

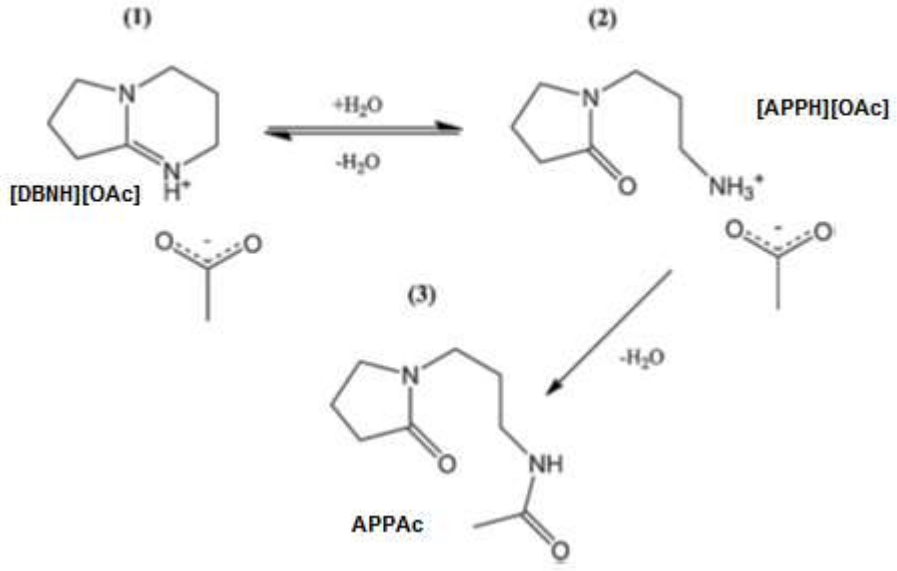

Figure 1. [DBNH][OAc] hydrolysis and decomposition reactions. Ahmad et al. (2016)

2. Thin film evaporator

Thin film evaporator is usually a vertical cylinder with heated walls. Liquid is spread on the metal wall at the top and it flows down the heated surface where evaporation happens. Pressure drop inside thin film evaporator is low and therefore the boiling point of the liquid only depends on its pressure and composition, not its position inside the evaporator. A vacuum pump can be added to perform the evaporation in low pressure. There are two main types of thin film evaporators, static thin film evaporator (STFE) and agitated thin film evaporator (ATFE). (Dziak, 2011)

In static film evaporator, or falling film evaporator (FFE), liquid is spread with a nozzle on the inner surface of the cylinder and it flows down the wall. Agitated thin film evaporator (ATFE), also called wiped film evaporator (WFE), uses rotating blades to spread and mix a thin layer of solution on cylindrical wall of the evaporator. Usually the layout is vertical and solution travels downwards on a helical path due to gravity and rotating blades. Lopez-Toledo (2006) notes that ATFE offers good conditions for evaporation of very viscous (up to 10^4 Pas) and thermally

unstable products. Mixture of water and [DBNH][OAc] is both viscous and thermally unstable, which makes ATFE a great option for its concentration. Blades ensure good mixing and turbulent conditions in the thin film, and short residence time helps handling of heat sensitive products (Vogel et al., 2014). The schematic of a vertical ATFE is presented in figure 2.

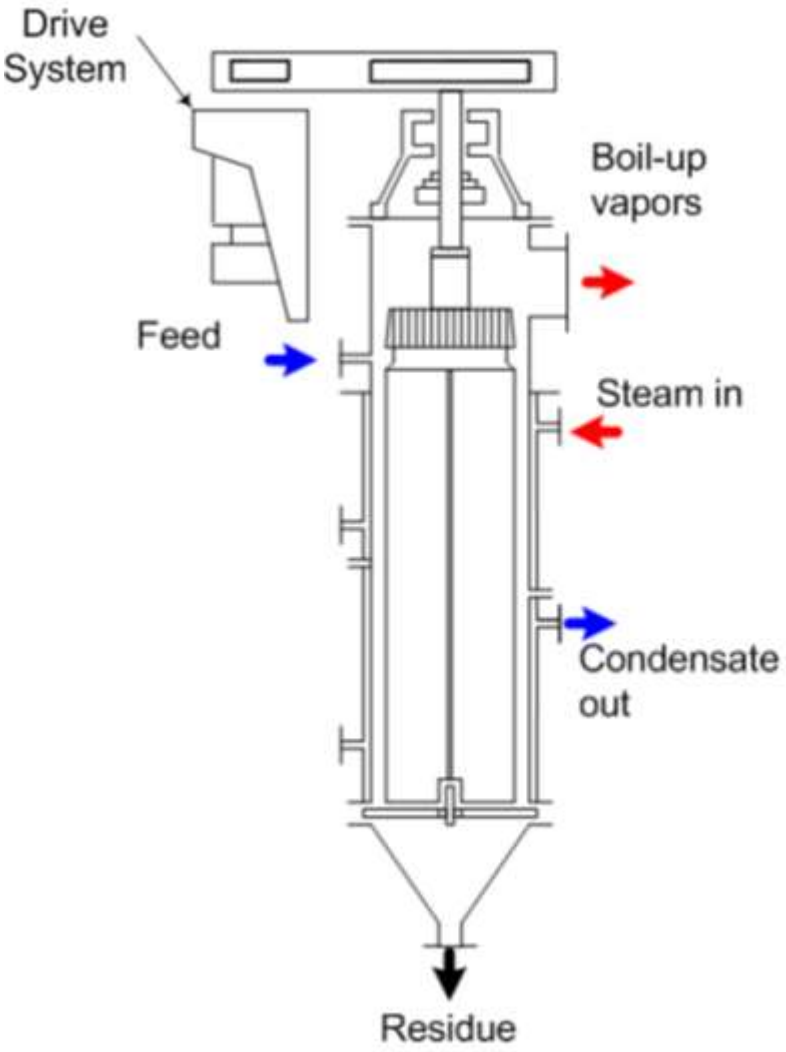

Figure 2. Vertical agitated thin film evaporator. Vogel et al. (2014)

3. Heat and mass transfer in thin film evaporators

Thin film evaporator can be described as heat and mass exchanger. Heating liquid or steam transfers heat through the evaporator wall to the liquid falling down inside the evaporator. Particles in liquid phase evaporate and transfer to gas phase. Vapor moving up is in contact with the liquid film and some of it may transfer back to liquid phase, which results in rectification. Heat and mass transfer coefficients are needed to accurately model thin film evaporator. Heat transfer is well studied phenomena in both FFE and ATFE but there is a lack of studies on mass transfer in ATFE.

3.1. Heat transfer

Overall heat transfer coefficient U can be determined from experimental measurements or calculated with different correlations. Overall heat transfer coefficient calculated from process measurements can only be applied to existing evaporators because it includes evaporator geometry in it. Lopez-Toledo (2006) gives equation for calculating U from process measurements:

$$U = \frac{Q}{A\Delta T_{ln}} \tag{1}$$

Total transferred heat can be calculated from the measurements of liquid and vapor and heating fluid entering and exiting the evaporator.

The subject of calculating heat transfer coefficients is widely studied and Lopez-Toledo (2006) has compiled theory of heat transfer in thin film evaporator and methods of heat transfer calculations in his paper. Overall heat transfer in thin film evaporator is dependent on three resistances. First is the external resistance between heating fluid, usually steam or oil, and the surface of the evaporator wall. Second is the resistance in the wall and third is the internal resistance between fluid inside and the heat transfer surface. These resistances are presented in figure 3.

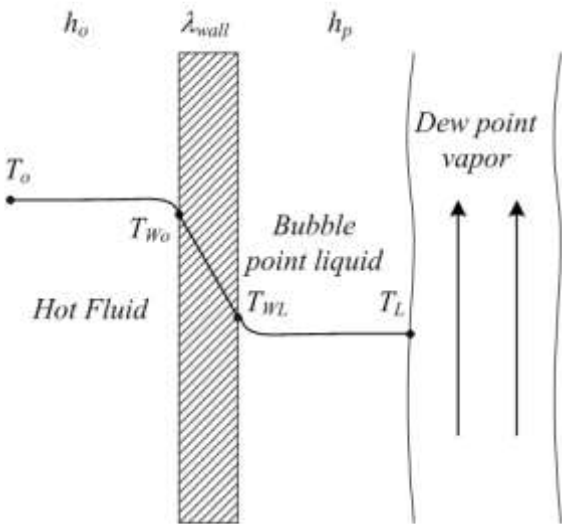

Figure 3. Resistances in agitated thin film evaporator. Lopez-Toledo (2006)

The equation for calculating U from different heat transfer coefficients is:

$$\frac{1}{U} = \frac{1}{h_o} + \frac{\delta_{wall}}{\lambda_{wall}} + \frac{1}{h_p} \tag{2}$$

If steam is used as heating fluid, the equation for external HTC calculation is (Lopez-Toledo 2006):

$$h_o = \frac{4}{3}\left(\frac{\lambda_s^3 \rho_s^2 g}{3\mu_s \Gamma}\right)^{\frac{1}{3}} \tag{3}$$

Where Γ= steam mass flow per unit length (kg/ms)

When using other heating fluid, couple of different equations are used depending on the flow characteristics. If the flow is laminar (Re<2100), Lopez-Toledo suggests equations from Sieder (1936):

$$Nu = \frac{h_o D}{\lambda} = 1.86 n_1^{-\frac{1}{3}} \left(\frac{\mu}{\mu_w}\right)^{0.14} \tag{4}$$

$$n_1 = \frac{\pi \lambda L}{4wC_p} \tag{5}$$

where w= hot fluid flow rate (kg/s)

Knudsen et al. (1997) give equations for calculating the Nusselt number in case of transition region and turbulent flow. When hot fluid flow is in transition region (2000 < Re < 10000) state then the Hausen equation can be used:

$$Nu = 0.116\left(Re^{\frac{2}{3}} - 125\right)\mathrm{Pr}^{\frac{1}{3}}\left[1 + \left(\frac{D}{L}\right)^{\frac{2}{3}}\right]\left(\frac{\mu}{\mu_w}\right)^{0.14} \tag{6}$$

In case of turbulent flow, Nu can be calculated with Dittus-Boelter equation:

$$Nu = 0.0243Re^{0.8}\mathrm{Pr}^{0.4}\left(\frac{\mu}{\mu_w}\right)^{0.14} \tag{7}$$

3.1.1. Internal heat transfer in ATFE

For internal heat transfer coefficient h_p there are many different correlations. Heat transfer is affected by agitation, so various equations have to be used in case of FFE and ATFE.

Bott and Romero (1963) ran tests with water and water-glycerol mixtures in an agitated thin film evaporator and developed an equation for the Nusselt number Nu:

$$Nu = 0.018Re_f^{0.46}Re_N^{0.6}\mathrm{Pr}^{0.87}\left(\frac{D}{L}\right)^{0.48}N_b^{0.24} \tag{8}$$

where N_b= number of blades in the evaporator

Bott and Sheikh (1966) later developed their correlation for Nu:

$$Nu = 0.65Re_f^{0.25}Re_N^{0.43}\mathrm{Pr}^{0.30}N_b^{0.33} \tag{9}$$

Both these correlations were developed with water-glycerol mixtures. Bott and Sheikh used more datapoints for water-glycerol mixture, and In a study by Lopez-Toledo (2006) equation 9 by Bott and Sheikh was determined to be more accurate than the earlier equation 8 by Bott and Romero.

Equations for calculating the dimensionless numbers are:

$$Nu = \frac{h_p D}{\lambda} \tag{10}$$

$$Re_f = \frac{4F}{\pi D \mu} \tag{11}$$

$$Re_N = \frac{D^2 N \rho}{\mu} \tag{12}$$

where N = rotational speed of the blades

$$Pr = \frac{C_p \mu}{\lambda} \tag{13}$$

3.1.2. Internal heat transfer in FFE

Numrich (1995) developed equation for calculating Nusselt number in FFE with turbulent flow. Comparison between measured and calculated data showed that the equation is accurate with Prandtl numbers up to 50:

$$Nu_L = 0.003 Re_f^{0.44} \mathrm{Pr}^{0.4} \tag{14}$$

Ahmed and Kaparthi (1963) performed measurements with water and water-glycerol solutions. Experiments were done with wide range of Re and Pr (3<Re<10250 and 3.6<Pr<950). Their equation is:

$$Nu_L = 0.00692 Re_f^{0.345} Pr^{0.4} \quad (15)$$

The Nusselt number in these two cases is calculated with equation:

$$Nu_L = \frac{h_p v^{\frac{2}{3}}}{\lambda g^{\frac{1}{3}}} \quad (16)$$

3.2. Mass transfer

Many mass transfer correlations have been developed for FFE but the situation with ATFE is very different. According to Lopez-Toledo (2006) and Rossi (2015) there is no suitable correlation for calculating mass transfer coefficients in ATFE. This problem can be avoided with analogy between heat and mass transfer, which will be discussed in chapter 3.2.2.

3.2.1. Mass transfer in FFE

Yih et al. (1982) studied O_2 and CO_2 absorption in water in wetted wall column. They compiled their experimental results with results from 10 other authors and developed correlations for liquid side mass transfer coefficient with different Reynolds number limitations:

$$k_L^{FFE} = 0.01099 Re_f^{0.31955} Sc^{\frac{1}{2}} \quad \text{When } 49 > Re > 300 \quad (17)$$

$$k_L^{FFE} = 0.02995 Re_f^{0.2134} Sc^{\frac{1}{2}} \quad \text{When } 300 > Re > 1600 \quad (18)$$

$$k_L^{FFE} = 0.09777 Re_f^{0.6804} Sc^{\frac{1}{2}} \quad \text{When } 1600 > Re > 10500 \quad (19)$$

$$Sc = \frac{\nu}{D} \tag{20}$$

3.2.2. Mass transfer in ATFE

Since heat and mass transfers are analogous in many cases, Lopez-Toledo (2006) and Rossi (2015) used the analogy to calculate mass transfer coefficient for ATFE. The so-called enhancement factor was used to describe the difference in heat transfer between FFE and ATFE.

$$\beta_h = \frac{h_p^{ATFE}}{h_p^{FFE}} \tag{21}$$

Mass transfer was assumed to be enhanced with same ratio as the heat transfer and thus mass transfer coefficient for ATFE could be calculated with equations developed for FFE.

$$k_L^{ATFE} = \beta_h k_L^{FFE} \tag{22}$$

Lopez-Toledo (2006) compared calculated overall heat transfer coefficients with and without mass transfer to experimental data. Results show that calculated results are more accurate when mass transfer is considered, which would suggest that heat-mass transfer analogy can be used. Results are shown in figures 4 and 5 where experimental and predicted overall heat transfer coefficients are compared.

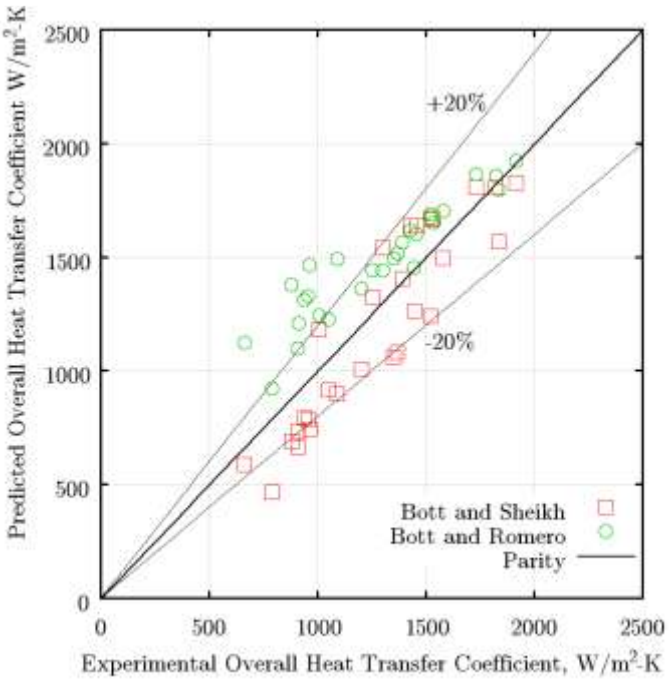

Figure 4. Calculated and measured heat transfer coefficients. Mass transfer not included. Lopez-Toledo (2006)

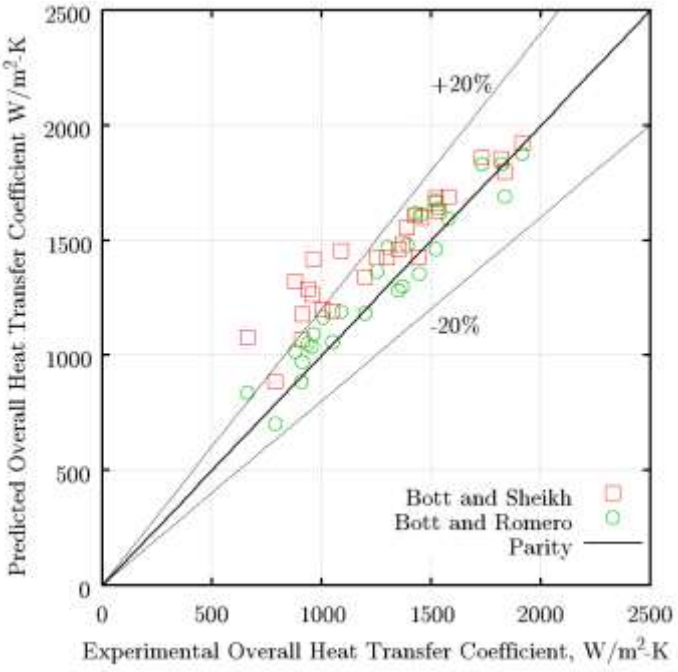

Figure 5. Calculated and measured heat transfer coefficients. Mass transfer included. Lopez-Toledo (2006)

4. TFE models

Various models have been developed to simulate the behavior of thin film evaporator. Some authors used steady-state simulator programs such as Aspen Plus, others developed equations for mass, energy and momentum balances which were solved with mathematical programs. This study focuses on studies that could give guidelines for appropriate models to be used for simulation of [DBNH][OAc]-water mixture evaporation with ATFE.

4.1. Batch distillation model

One basic theory for calculating thin film evaporator efficiency is called Billet's theory. Billet made a mass balance equation for more volatile component on small dh length of the evaporator (see figure 6). This is similar to the equation used in batch distillation. It is assumed that the produced vapor is in equilibrium with the liquid and it exits the evaporator without any contact with liquid phase. Dziak (2011) presents the equations behind Billet's theory in his article about mass and heat transfer in thin-film evaporation.

$$\dot{L} \cdot x = \left(\dot{L} - d\dot{V}\right) \cdot (x - dx) + y^* d\dot{V} \tag{23}$$

Where $\dot{L}$= Liquid molar flow at the inlet of the element dh

$\dot{L} - d\dot{V}$= Liquid molar flow at the outlet of the element dh

$x - dx$= Concentration of the more volatile component in liquid at the outlet of dh

y^*= Concentration of the more volatile component in vapor

This equation can be integrated and the result is equation 24:

$$\ln \frac{\dot{L}_F}{\dot{L}_R} = \int_{x_R}^{x_F} \frac{dx}{y^* - x} \tag{24}$$

Equation 24 allows residue flowrate $\dot{L}_R$ to be solved when feed flowrate $\dot{L}_F$, feed concentration x_F, residue concentration x_R and vapor liquid equilibrium data is known. Afterwords the distillate concentration can be calculated from mass balance equations.

$$\dot{D} = \dot{L_F} - \dot{L_R} \tag{25}$$

$$x_D = \frac{\dot{L_F} \cdot x_F - \dot{L_R} \cdot x_R}{\dot{D}} \tag{26}$$

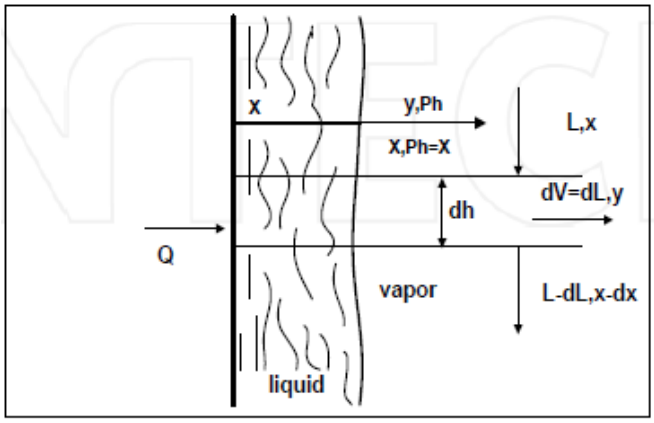

Figure 6. Billet's theory for two-component liquid thin film evaporation. Dziak (2011)

After presenting the theory Dziak (2011) focused on determining whether or not mass transfer resistances existed in thin film evaporation and how well Billet's theory would perform. He conducted measurements in laboratory-scale FFE and ATFE with varying rotating speed and heat load. Mixtures of water-propylene glycol and water-isopropanol were used. Results are shown in figures 7 and 8.

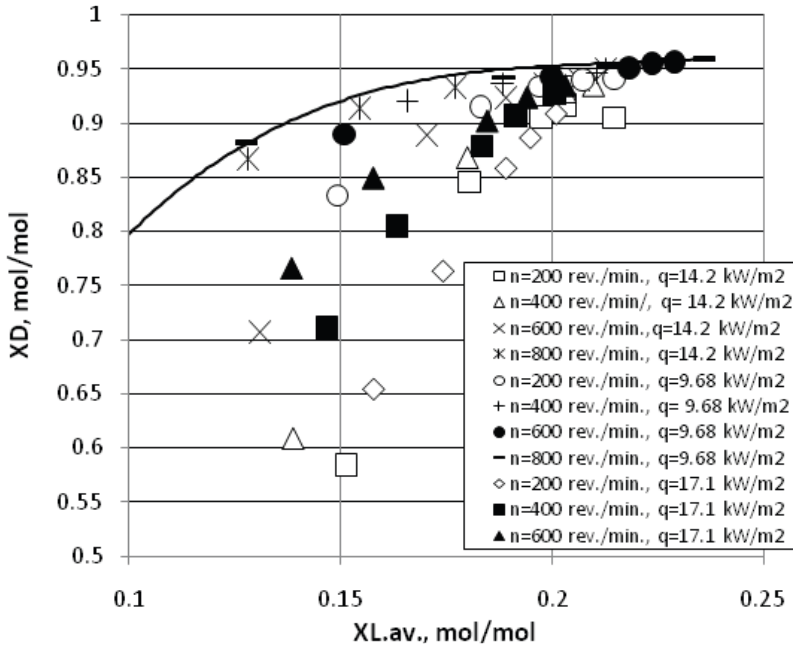

Figure 7. Theoretical evaporation result in solid line and experimental measurements in dots. ATFE with water-propylene glycol solution feed. X(D) is the mole fraction of water in distillate, X(L) is mole fraction of water in feed. Dziak (2011)

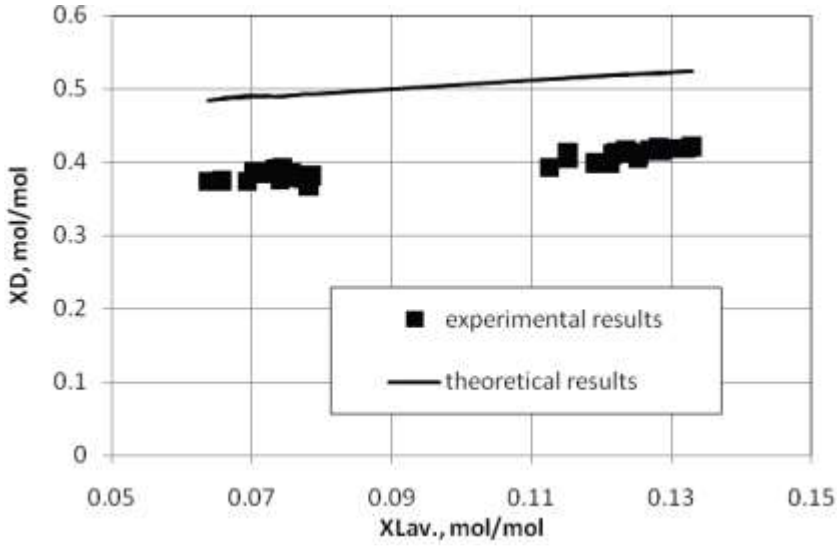

Figure 8. Theoretical and experimental evaporation results in FFE. Falling film evaporator with water-isopropanol solution feed. X(D) is the mole fraction of isopropanol in distillate, X(L) is mole fraction of isopropanol in feed. Dziak (2011)

From figures 7 and 8 it can be concluded that the liquid side mass transfer resistances affect the process of evaporation, especially with FFE. This suggests that in most cases simple equilibrium model cannot be used to simulate evaporation accurately. However, Dziak (2011) noted that in the case of agitated thin film evaporator, moderate heat load and high blade rotational speed, experimental measurements are close to theoretical calculations. This can be seen in figure 7, the experimental results marked with asterisk (*) and minus sign (-) are close to theoretical results.

4.2. Single equilibrium-stage flash model

The possibility of ionic liquid recycling by thermal evaporation was studied by Ahmad et al. (2016). In their paper evaporation of [DBNH][OAc] with ATFE was studied and measurements were made for VLE data of the chemical system. The results showed negative deviation from Raoults law for [DBNH][OAc]. It was assumed that at low pressure and temperatures below 373 K the ionic liquid-water mixture could be modelled as binary mixture. Data regression in Aspen Plus was used to determine the binary interaction parameters for NRTL model from the experimental data. The phase equilibrium diagram produced by NRTL model for two different temperatures is presented in figure 9.

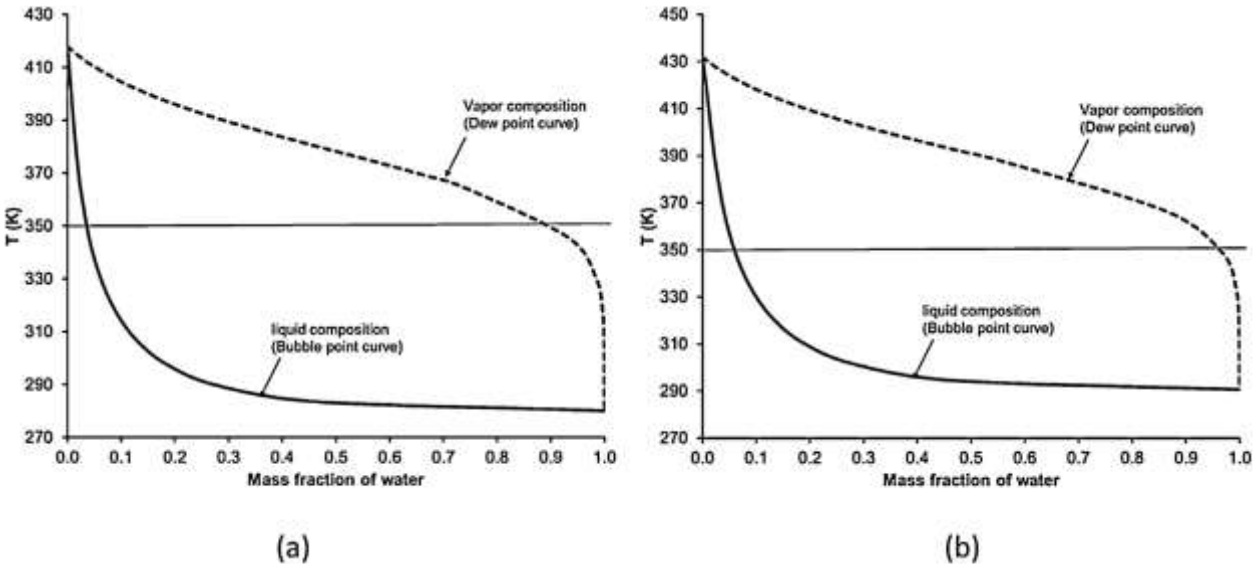

Figure 9. Phase diagram produced by NRTL model. a = 1 kPa, b = 2 kPa. Ahmad et al. (2016)

ATFE was simulated in Aspen Plus with rigorous two-phase flash model. Isothermal flash temperature was determined to be the same as heating jacket temperature and system temperature was used as the flash temperature. 9 experiments were run with different operating conditions and feed flowrates with ATFE and the same conditions were used in simulations. Comparison of simulation and experimental water concentrations in residue is presented in figure 10. It shows that the simulation is reasonably accurate but better accuracy could be achieved with other assumptions. For example, the use of heating jacket temperature as the flash temperature is not completely accurate because the temperature of the inside wall of the evaporator is different from the heating jacket temperature. Ahmad et al. (2016) concluded that better simulation results could be achieved with more rigorous models.

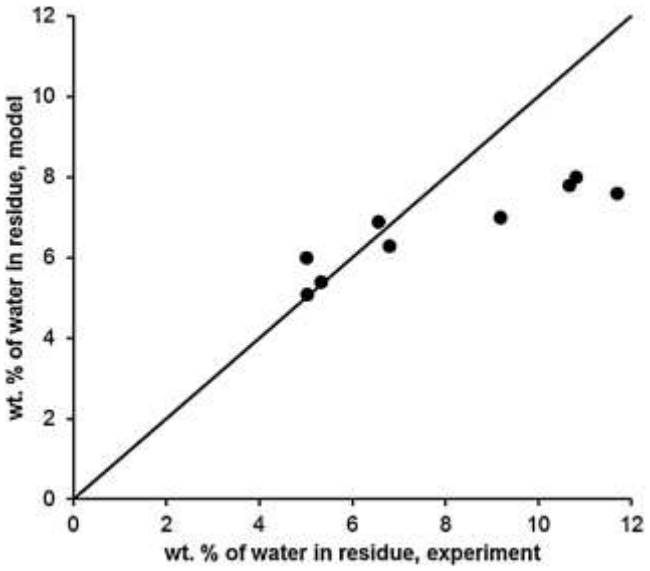

Figure 10. Simulation vs experimental results. Ahmad et al. (2016)

4.3. Rigorous heat exchanger-flash model

Chawankul et al. (2001) developed an Aspen Plus simulation model for concentrating orange juice in agitated thin film evaporator. Their work was based on earlier work on concentrating sugar syrup done by Chuaprasert et al. (1999). The model consisted of a two-phase heat exchanger and a flash drum which together represent the agitated thin film evaporator. Orange juice was fed to the heat exchanger which was heated by steam. The flash drum with the same pressure as the heat exchanger was then used to separate the two-phase mixture of vapor and concentrated orange juice. Adiabatic operation was assumed in flash column because its purpose was only to separate the two phases.

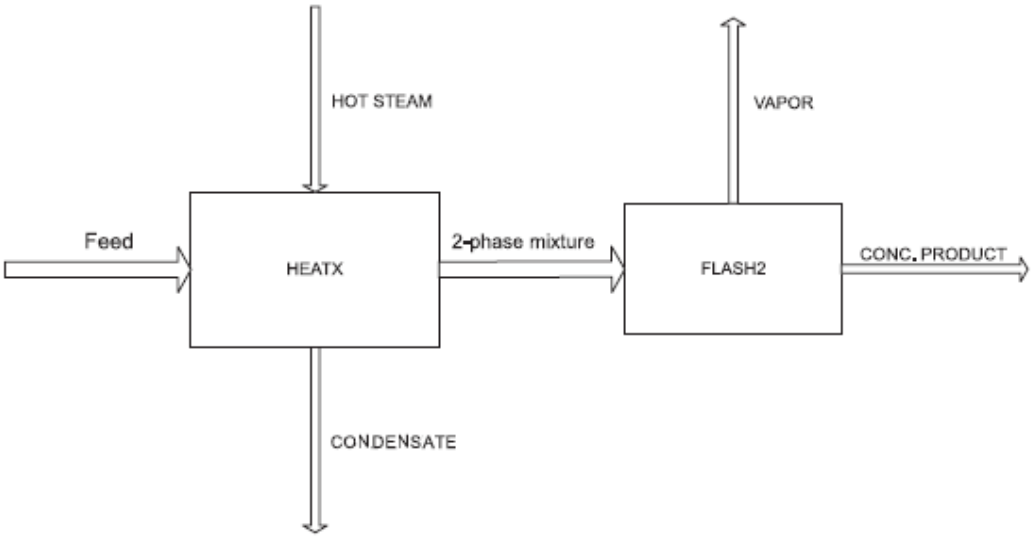

Figure 11. Aspen Plus simulation model with heat exchanger and flash column. Chuaprasert et al. (1999)

The heat exchanger was specified with heat transfer area A and overall heat transfer coefficient U. Chawankul et al. (2001) used equations developed by Sae Tae (1999) to calculate U. These calculations required thermo-physical properties of orange juice, which were modelled as functions of temperature and solid content developed from experimental data. Equations from Sae Tae (1999) were however developed for sugar syrup and their applicability to orange juice was not certain. Therefore, U was also determined from direct measurements as discussed in chapter 3.1 in this paper. This is called effective heat transfer coefficient.

Chawankul et al. (2001) conducted 13 experiments, 8 with lab scale evaporator (batches 1-8) and 5 with pilot scale one (batches 9-13). The results were compared to simulations with calculated (figures 12-14) and effective (figures 15-17) heat transfer coefficients. Figures 12 and 13 show that simulated flowrates are of reasonably good accuracy with laboratory scale and somewhat worse with pilot scale experiments. Figure 14 shows large difference in product composition with batches 5-7. Authors speculated that this could be a result of scalding of the orange juice on the heat transfer surface due to very low feed flowrates in the mentioned batches.

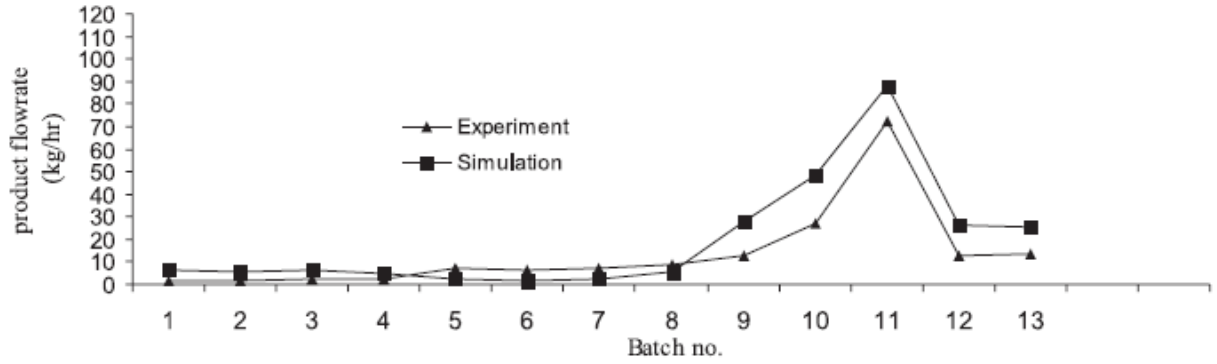

Figure 12. Product flowrate, experimental vs simulation with calculated U. Chawankul et al. (2001)

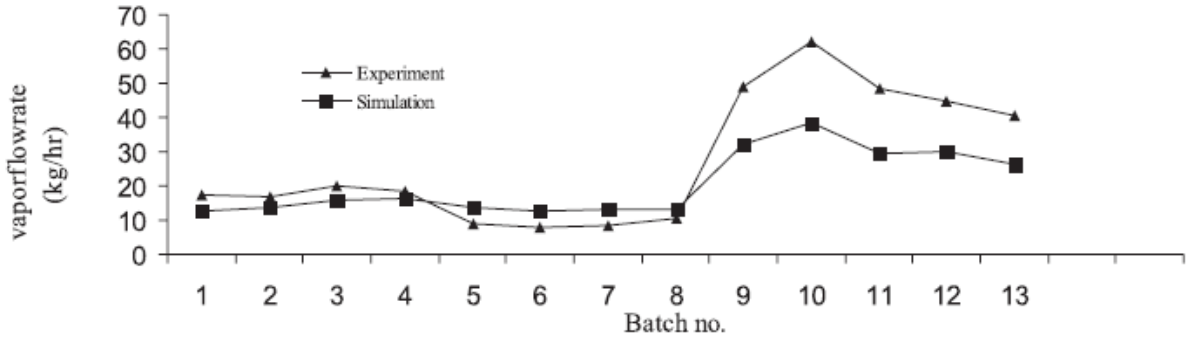

Figure 13. Vapor flowrate, experimental vs simulation with calculated U. Chawankul et al. (2001)

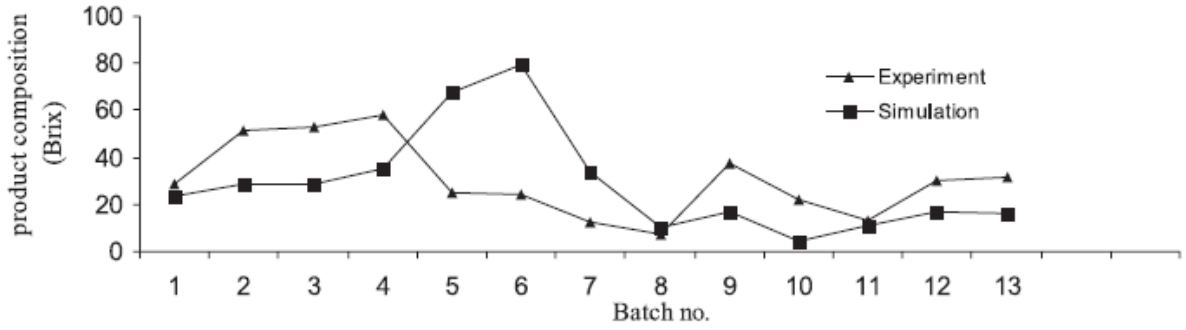

Figure 14. Product composition, experimental vs simulation with calculated U. Chawankul et al. (2001)

Next Chawankul et al. (2001) reconciled the experimental data to lower the effect of random and possible gross errors in measurements. Aspen Plus was used to reconcile the data to satisfy energy and mass balance equations. The reconciled data was compared to simulation with effective heat transfer coefficient and direct experimental data. Figures 15-17 show that simulation results with effective heat transfer coefficient are more accurate than simulation with calculated U and agree well with experimental data with the exception of batches 5-7. The simulation results are also closer to reconciled data than the raw experimental data. Chawankul et al. (2001) conclude that the reconciliation improved the fit between simulation and experimental data by 60 % on average.

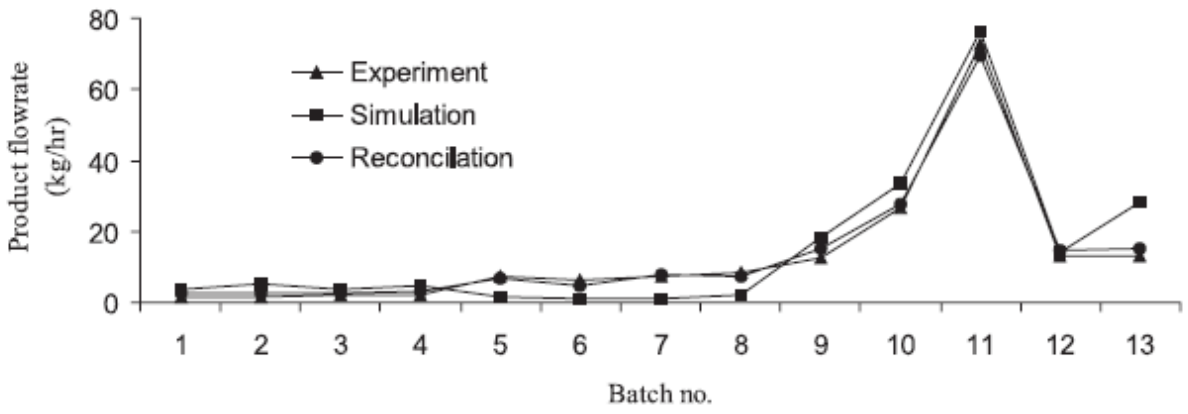

Figure 15. Product flowrate, experimental vs recinciliation vs simulation with effective U. Chawankul et al. (2001)

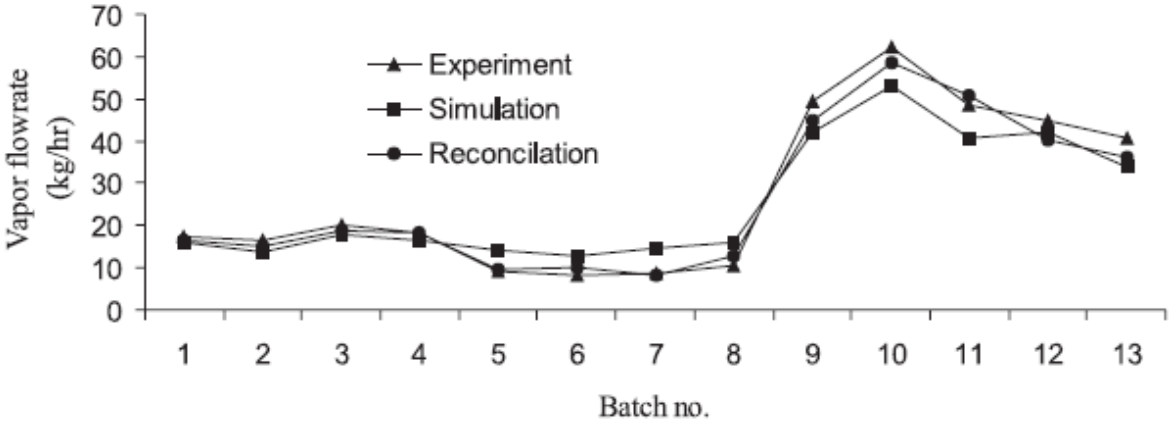

Figure 16. Vapor flowrate, experimental vs recinciliation vs simulation with effective U. Chawankul et al. (2001)

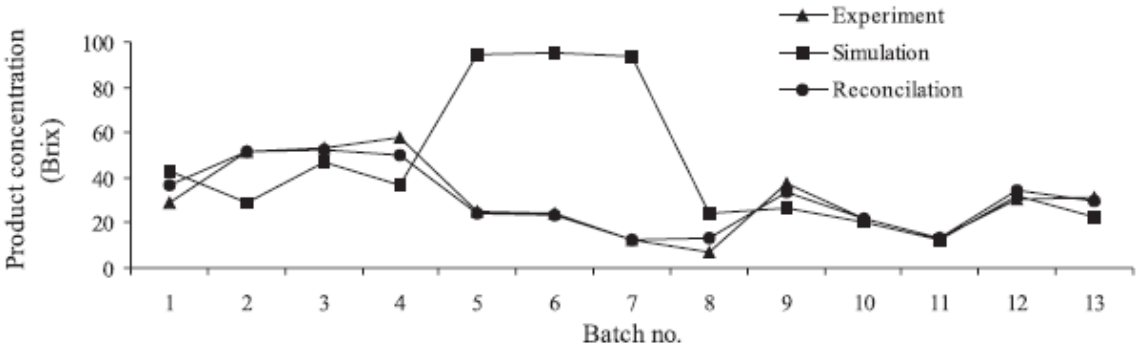

Figure 17. Product composition, experimental vs recinciliation vs simulation with effective U. Chawankul et al. (2001)

4.4. Equilibrium multistage model

Equilibrium multistage models can also be used to model thin film evaporator. Schaal (2008) constructed equilibrium multistage models in Aspen Plus and compared their results to experimental data to verify the accuracy of those models.

Two different models were used, an open evaporation and a closed evaporation. In the open evaporation, the assumption was made that the vapor leaving the stage without interaction with the liquid. This open evaporation model approaches the batch model presented earlier in chapter 4.1. In the closed evaporation vapor travelling up was assumed to be in contact with the

falling liquid. Liquid was fed on the top stage, as feed in thin film evaporation would be at the top of the evaporator. Parameters for simulation were feed flowrate and composition, heat load on each stage and evaporation rate (ER). ER is the ratio between head flow (produced vapor) and feed flow. Heat load on each stage was set to be the same. Both models are presented in figure 18. The models were run with two different liquid solutions; water-ethylene glycol and methanol-water.

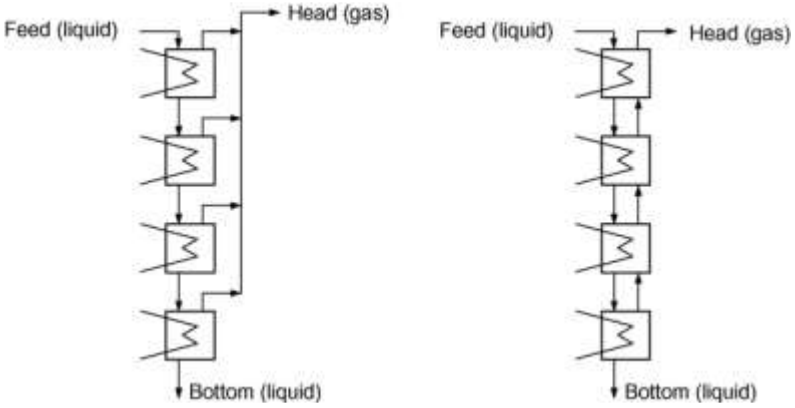

Figure 18. Examples of open(left) and closed(right) multistage models. (Schaal 2008)

Simulations were run with different number of stages. Results presented in figure 19 show, as expected, that evaporation efficiency is better with multiple stages and multi-stage simulations are more accurate to experimental data than single stage simulation. Closed evaporation models gave higher evaporator efficiency results.

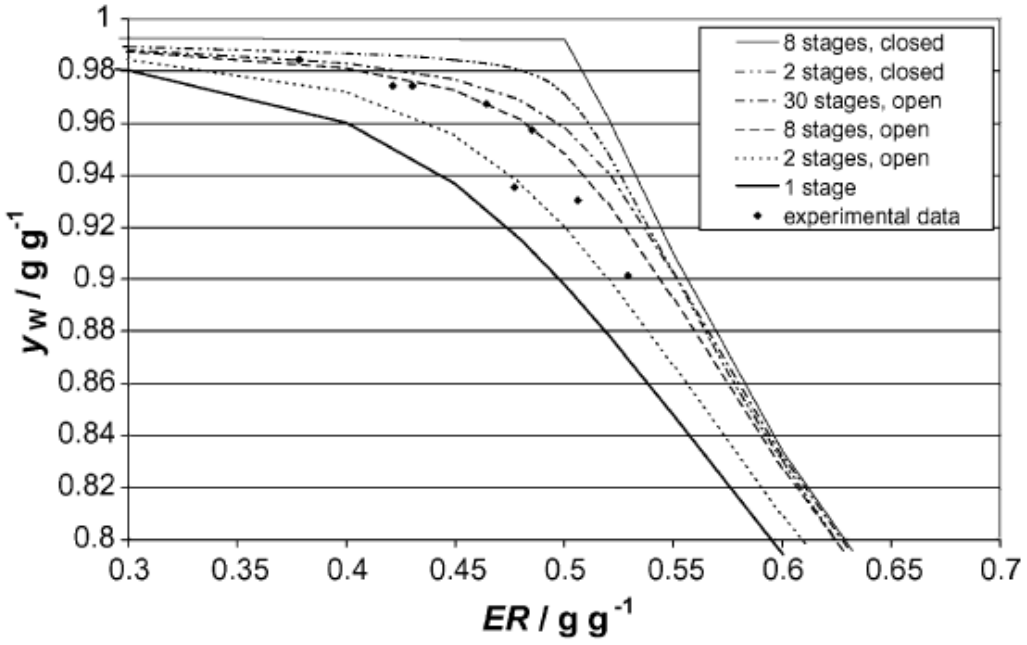

Figure 19. Water-ethylene glycol evaporation. Experimental and simulation results. Schaal (2008)

Eight-stage model was chosen for further comparison and simulations were done with different feed concentrations. In case of water-ethylene glycol solution the open stage model performed more accurately than the closed stage model when compared to experimental results (figures 20 and 21). With methanol-water system the closed stage model was more accurate when evaporation rate and feed water concentration were low, as can be seen in figure 23.

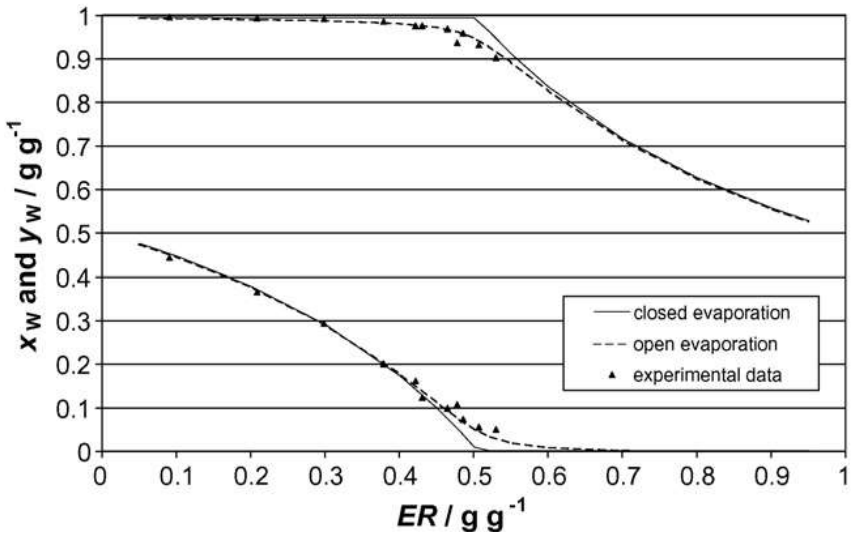

Figure 20. Water-ethylene glycol, x(F, water)=0.5, p=10 kPa. Schaal (2008)

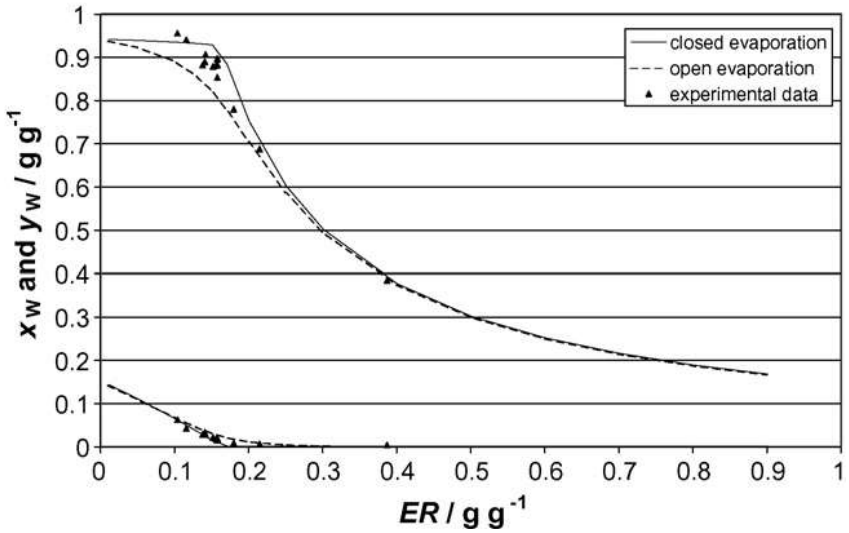

Figure 21. Water-ethylene glycol, x(F, water)=0.15, p=10 kPa. Schaal (2008)

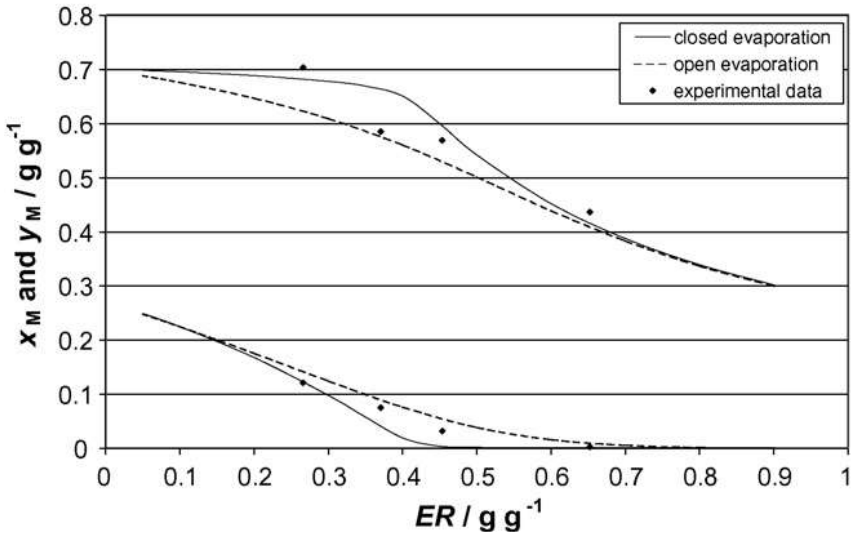

Figure 22. Methanol-water, x(F, methanol)=0.5, p=40 kPa. Schaal (2008)

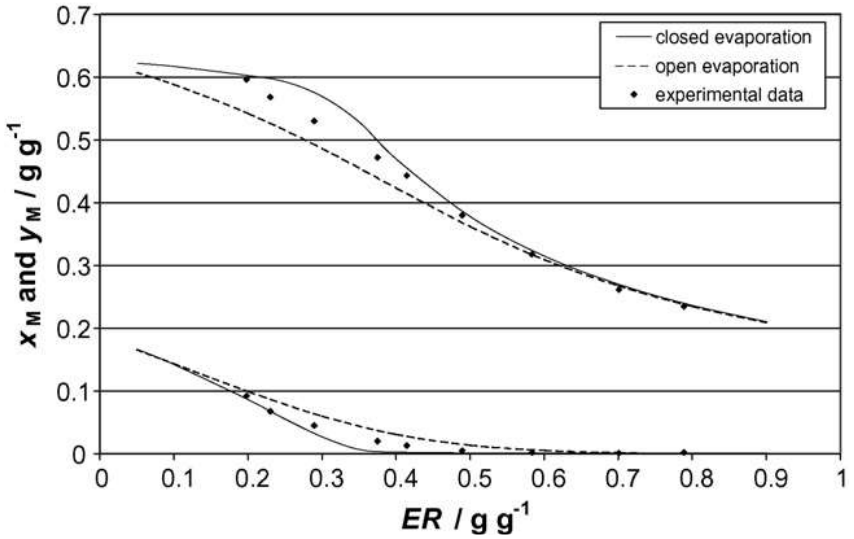

Figure 23. Methanol-water, x(F, methanol)=0.188 p=10 kPa. Schaal (2008)

Results suggest that thin film evaporation can be simulated with equilibrium multistage model. Open stage model is better with the exception of low evaporation rates and feed concentrations. This can be explained with rectification. Small vapor flow results in longer contact time with liquid which leads to better separation efficiency. Schaal (2008) suggests that with evaporation

ratios of 0.1-0.2 closed stage model should be used and with higher evaporation rates open stage model should be preferred.

4.5. Non-equilibrium dynamic model

Rossi et al. (2015) developed a non-equilibrium dynamic model for simulation ATFE. The scope was to develop a model that can predict the effect of the changes of operating and boundary conditions to evaporator performance. Their stage-wise model was based on the following six assumptions. i) Every stage is considered as a continuous stirred tank reactor because of rotating blades. ii) No backmixing is present inside the evaporator. iii) Variables entering each stage are equal to the variables leaving the previous stage. iv) Flat plate assumption for diffusion is made, because the film thickness is very little compared to the reactor diameter. v) Interface concentration of the evaporating substance is the equilibrium concentration in the conditions of the stage. vi) Vapor-phase is considered pseudo-stationary.

With these assumptions, Rossi et al. (2015) developed material, energy and momentum balances for the evaporator.

$$\frac{d\omega_{i,n}^{L}}{dt} = \frac{\rho_{mix,n-1}^{L} A_{n-1}^{L} v_{n-1}^{L}}{\rho_{mix,n}^{L} V_{n}^{L}} \left(\omega_{i,n-1}^{L} - \omega_{1,n}^{L}\right) + \frac{A_{n}^{LV}}{\rho_{mix,n}^{L} V_{n}^{L}} \left(J_{i,n}^{LV} - \omega_{i,n}^{L} \sum_{i=1}^{NC} J_{i,n}^{LV}\right) \tag{27}$$

$$0 = \rho_{mix,n+1}^{V} A_{n+1}^{V} v_{n+1}^{V} \omega_{i,n+1}^{V} - \rho_{mix,n}^{V} A_{n}^{V} v_{n}^{V} \omega_{i,n}^{V} - A_{n}^{LV} J_{i,n}^{LV} \tag{28}$$

$$\frac{dV_{n}^{L}}{dt} = -\frac{V_{n}^{L}}{\rho_{mix}^{L}} \frac{d\rho_{mix,n}^{L}}{dt} + \frac{\rho_{mix,n-1}^{L}}{\rho_{mix,n}^{L}} A_{n-1}^{L} v_{n-1}^{L} - A_{n}^{L} v_{n}^{L} + \frac{A_{n}^{LV}}{\rho_{mix,n}^{L}} \sum_{i=1}^{NC} J_{i,n}^{LV} \tag{29}$$

$$0 = \rho_{mix,n+1}^{V} A_{n+1}^{V} v_{n+1}^{V} - \rho_{mix,n}^{V} A_{n}^{V} v_{n}^{V} - A_{n}^{LV} \sum_{i=1}^{NC} J_{i,n}^{LV} \tag{30}$$

$$0 = \rho_{mix,n}^{V} V_{n}^{L} g - \frac{1}{2} \rho_{mix,n}^{L} f_{n}^{LW} A^{LW} (v_{n}^{L})^{2} - \frac{1}{2} \rho_{mix,n}^{V} f_{n}^{LV} A^{LV} (v_{n}^{V} + v_{n}^{L})^{2} \tag{31}$$

Equations 27 and 28 are mass conservation balance equations for liquid and vapor for species i in stage n. Equations 29 and 30 are global material balance equations for liquid and vapor. Equation 31 is momentum balance equation for stage n. Enthalpy balance equations were developed for both evaporating (eq. 32-33) and boiling (eq. 34-35). Vapor-liquid equilibrium model was used to determine the use of boiling or evaporating enthalpy balance equations in each stage.

$$dT_n^L = \frac{1}{\rho_{mix,n}^L V_n^L \sum_{i=1}^{NC} \omega_{i,n}^L c_{pi,n}^L}\Bigg[\rho_{mix,n-1}^L A_{n-1}^L v_{n-1}^L (T_{n-1}^L - T_n^L)\sum_{i=1}^{NC}\omega_{i,n}^L \frac{c_{pi,n-1}^L - c_{pi,n}^L}{2} + A_n^{LV}\sum_{i=1}^{NC} J_{i,n}^{LV}\frac{c_{pi,n}^L(T_n^L) - c_{pi,n}^L(T_n^V)}{2}(T_n^V - T_n^L) + A_n^{LV}h_n^{LV}(T_n^V - T_n^L) + A_n^{LW}U_n^{WV}(T_{steam} - T_n^L)\Bigg] \tag{32}$$

$$0 = \rho_{mix,n+1}^V A_{n+1}^V v_{n+1}^V (T_{n+1}^V - T_n^V)\sum_{i=1}^{NC}\omega_{i,n}^V \frac{c_{pi,n-1}^V - c_{pi,n}^V}{2} - A_n^{LV}\sum_{i=1}^{NC} J_{i,n}^{LV}\frac{c_{pi,n}^L(T_n^L) - c_{pi,n}^L(T_n^V)}{2}(T_n^V - T_n^L) - A_n^{LV}h_n^{LV}(T_n^V - T_n^L) \tag{33}$$

$$0 = \frac{1}{\rho_{mix,n}^L V_n^L \sum_{i=1}^{NC} \omega_{i,n}^L c_{pi,n}^L}\Bigg[\rho_{mix,n-1}^L A_{n-1}^L v_{n-1}^L (T_{n-1}^L - T_n^L)\sum_{i=1}^{NC}\omega_{i,n}^L \frac{c_{pi,n-1}^L - c_{pi,n}^L}{2} + A_n^{LV}J_n^{TOT}\sum_{i=1}^{NC}\omega_{i,n}^{V,eq}\Delta h_{i,n}^{ev}(T_n^L) + A_n^{LV}h_n^{LV}(T_n^V - T_n^L) + A_n^{LW}U_n^{LW}(T_{steam} - T_n^L)\Bigg] \tag{34}$$

$$0 = \rho^V_{mix,n+1} A^V_{n+1} v^V_{n+1} (T^V_{n+1} - T^V_n) \sum_{i=1}^{NC} \omega^V_{i,n} \frac{c^V_{pi,n-1} - c^V_{pi,n}}{2} - A^{LV}_n J^{TOT}_n \sum_{i=1}^{NC} \omega^{V,eq}_{i,n} \Delta h^{ev}_{i,n}(T^L_n) - A^{LV}_n h^{LV}_n (T^V_n - T^L_n) \quad (35)$$

Further these equations requires a VLE model and heat and mass transfer coefficients. Rossi et al. (2015) used equations 3 and 9 mentioned in chapter 3 of this thesis to determine external and internal heat transfer coefficient. Heat and mass transfer analogy was used to determine mass transfer coefficient. Initial conditions (composition, temperature and flowrate of the feed) and boundary conditions were determined and differential algebraic system was solved with BzzMath numerical library.

To test the model, a case study was conducted on evaporation of a sucrose aqueous solution, results are presented in figures 24 and 25. Rossi et al. (2015) concluded that further validation of the model with comparison to experimental data is needed and would be done in future works.

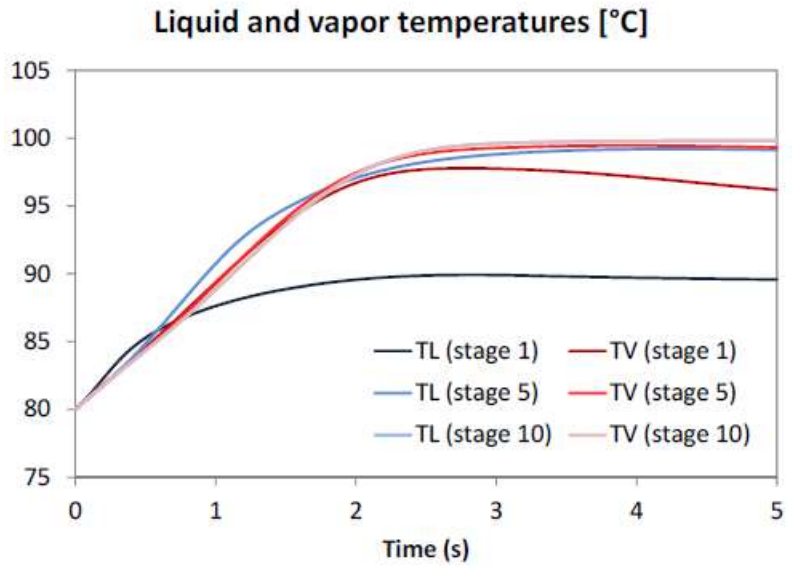

Figure 24. Temperatures of vapor and liquid inside ATFE over time. Rossi et al. (2015)

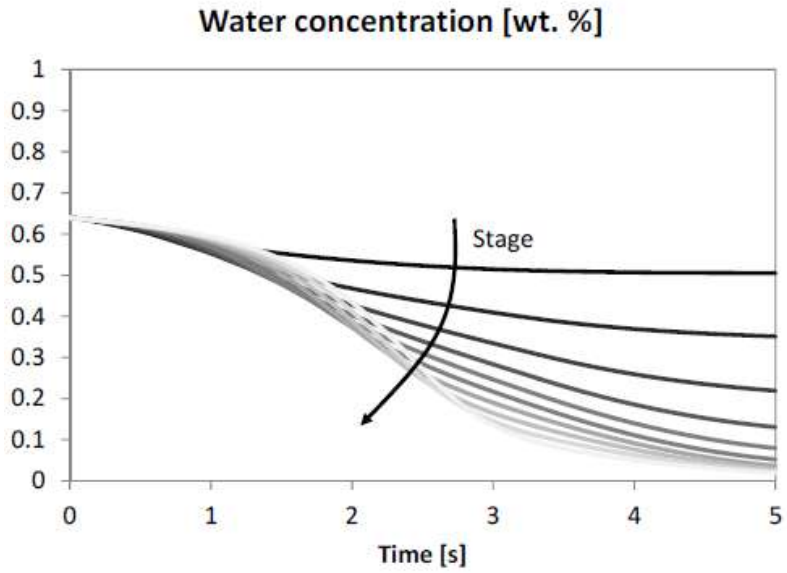

Figure 25. Water content on each stage in ATFE over time. Rossi et al. (2015)

.

APPLIED PART

In the applied part of this work, focus will be on modelling the thin film evaporator with a batch distillation model. The simple flash model does not consider the concentration change along the evaporator height and thus batch models could be able to model the ATFE more accurately. Rate based modeling could be even more accurate but due to its complexity and the lack of information on the properties and the reactions of ionic liquid it is not considered in this part.

Various models for simulating the evaporation of [DBNH][OAc]-water solution in ATFE were constructed in Aspen environment. The experimental results from Ahmad et al. (2016) were used to verify accuracy of the model. Binary NRTL parameters for [DBNH][OAc]-water mixture and vapor pressure correlation parameter for [DBNH][OAc] were taken from the flash model developed by Ahmad et al. (2016). A similar model based on flash was constructed and the results were used to compare the results to the batch model developed in this study.

5. Theory behind batch model

Flash model may give accurate results for ATFE if the temperature change inside the evaporator is low. In the case of [DBNH][OAc]-water mixture, the temperature rises fast as the concentration changes.

Pressures and temperatures in experiments by Ahmad et al. (2016) varied between 1.6-3.1 kPa and 77-94 °C. Feed concentration was 80 w-% water the rest being the ionic liquid. The boiling point of [DBNH][OAc]-water mixture depends highly on its concentration. In this specific pressure range, the boiling point of the feed varies between 14.6-25.3 °C. At 3.1 kPa the mixture with 80 w-% water content will start boiling at 25.3 °C and its boiling point rises, as the mixture gets more concentrated.

In the evaporator at 3.1 kPa and with heating jacket temperature at 77 °C, the feed will start boiling at 25.3 °C. If enough heating power is provided, the bottom product will be very close to the heating jacket temperature 77 °C. The vapor production inside the evaporator takes place from 25.3-77 °C with varying composition along the evaporator height. At high evaporation ratios, the vapor flow will be fast. This enables the assumption that the vapor does not go to the

equilibrium with the liquid above it. Thus, the composition of the total produced vapor cannot be read from the VLE diagram at the heating jacket temperature. On the other hand, the bottom product composition can be estimated from the VLE diagram at heating jacket temperature. Txy-diagram for water-[DBNH][OAc] mixture at 3.1 kPa is presented in figure 26.

This evaporation behavior inside thin film evaporator resembles batch distillation and therefore the hypothesis is that a batch-type reactor model could give accurate results for the product compositions.

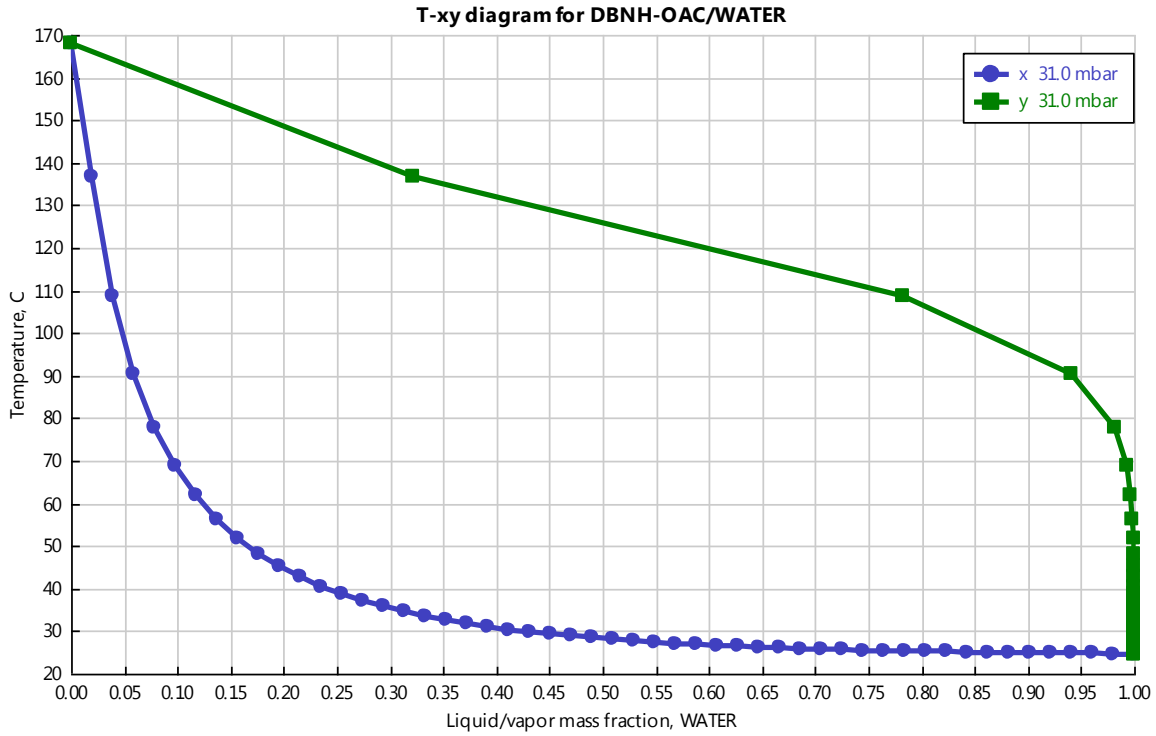

Figure 26. Txy-diagram for water/[DBNH][OAc] mixture at 3.1 kPa

5.1. Flash model

The flash models evaporation at single temperature and pressure with vapor and liquid concentrations at equilibrium. The model consists of a flash block with a single inlet for the feed mixture and the outlets for vapor and liquid. The model is illustrated in figure 27.

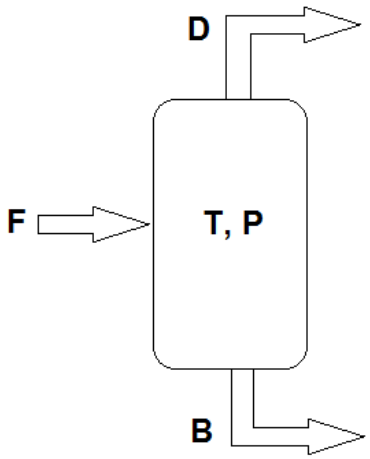

Figure 27. Illustration of the flash model.

The flash model was constructed in Aspen Plus V8.8. Its purpose was to function as a comparison for other models together with the already existing experimental data. Water/[DBNH][OAc] NRTL-parameters and vapor pressure correlation parameters for [DBNH][OAc] were taken from Ahmad et al. (2016). The parameters are presented in tables 1 and 2. Operation parameters were temperature and pressure of the flash and flowrate and composition of the inlet stream. Flash simulations were run at three different pressures with temperature range of 25-95℃. Feed concentration was 80 w-% water and 20 w-% [DBNH][OAc]. Results are presented in figures 28 and 29.

Table 1. Vapor pressure correlation parameters for Aspen simulation. Ahmad et al. (2016)

Vapor pressure correlation parameters for [DBNH][OAc]. $Ln[P(Pa)] = A + \frac{B}{T(K)+C}$		
A	B	C
28.289	-8933.6	0.0003197

Table 2. Binary interaction parameters for Aspen simulation. Ahmad et al. (2016)

Binary interaction parameters of NRTL model for water(1) and [DBNH][OAc] (2)				
a12	a21	b12	b21	α12=21
-0.78973	-6.28699	1337.985	550.334	0.2

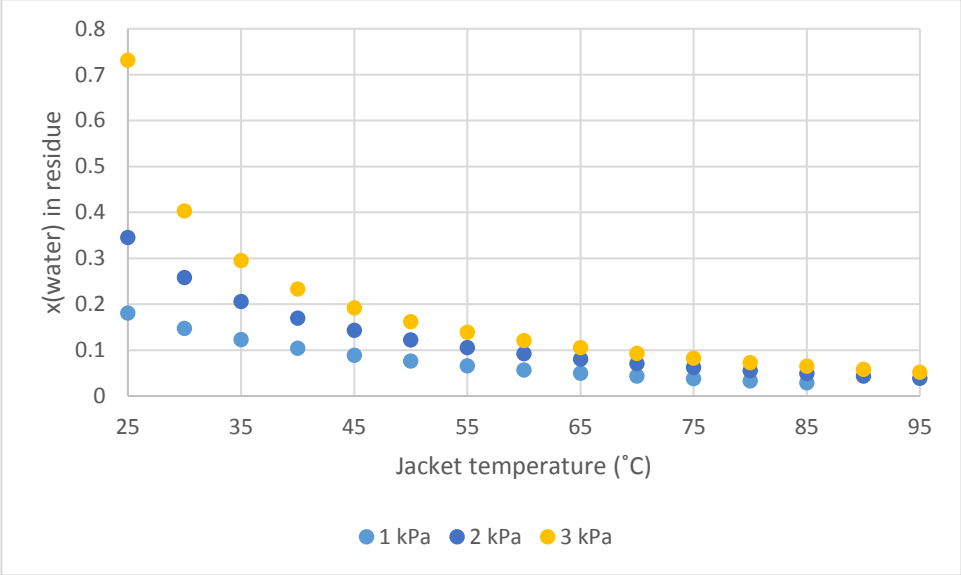

Figure 28. Mass fraction of water in residue. (Flash model)

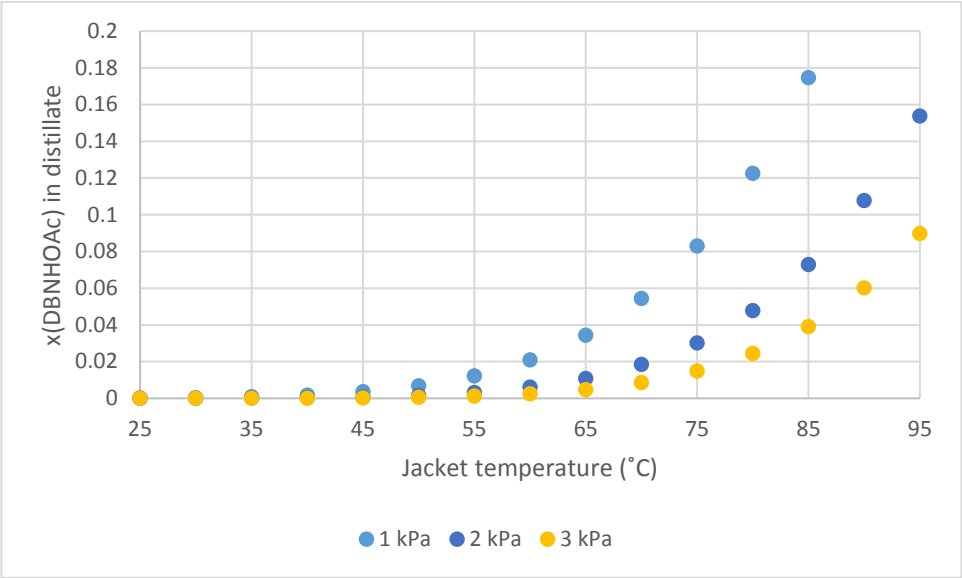

Figure 29. Mass fraction of [DBNH][OAc] in distillate. (Flash model)

5.2. Batch model

Batch distillation is time-dependent. Temperature and composition of the produced vapor changes as the temperature and composition of the evaporating liquid changes over time. Similar phenomenon occurs in a thin film evaporator as the properties of the liquid and the vapor changes, in this case over the evaporator height instead of over time. Figure 30 shows the similarities between the batch model and a real thin film evaporator. This thesis refers to models that consider this temperature change as batch models. When the batch distillation model is run from an initial temperature to the operating temperature of a thin film evaporator, it can give compositions for the produced vapor and liquid in an operating steady-state thin film evaporator. Composition of the total produced vapor in batch distillation is the same as the vapor produced in TFE. Composition of the liquid remaining in the pot of the batch distillation column is the same as the bottom product in TFE.

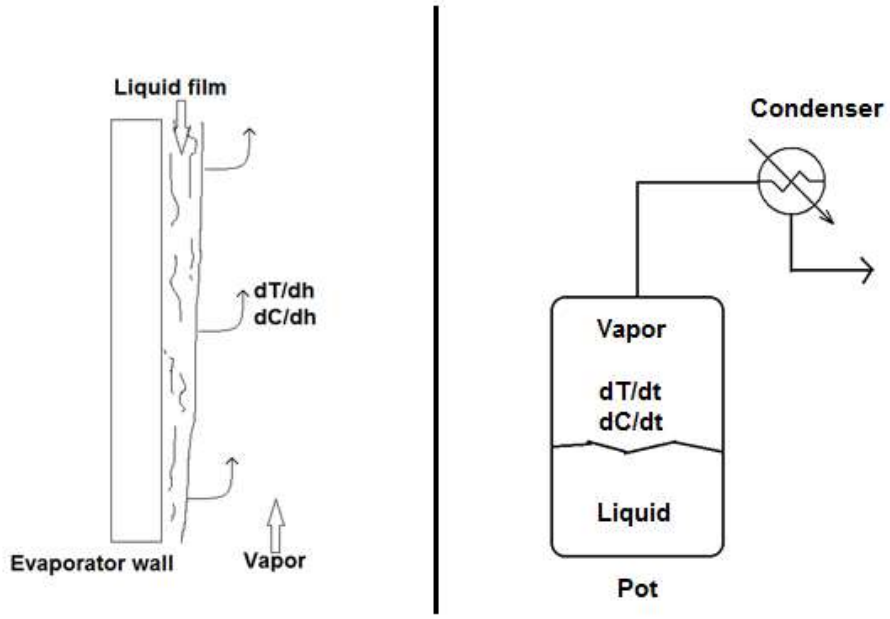

Figure 30. Left: Illustration of liquid and vapor inside a thin film evaporator. Right: Batch model.

The batch distillation model was constructed in Aspen Batch Model V8.8. Components were water and [DBNH][OAc], their properties were imported with Aspen Properties Desktop V8.8. [DBNH][OAc] was defined as a conventional component with user-defined parameters. Parameters were the same as in the flash model.

The model consisted of a pot with a condenser. Reflux rate was set to zero. The pot had an initial charge of water an [DBNH][OAc]. The mixture was heated and the produced vapor was condensed. Constant duty or constant heating fluid temperature had to be defined, constant heating temperature was used in this thesis. The temperature of the liquid in the pot was set as the end condition in the operation step. The program allowed the implementation of heat transfer coeffifcients, but it was not necessary because the purpose of this simulation was to get the concentrations and the temperatures of the residue and the total produced vapor. The simulation would then run until the liquid in the pot would reach the end condition temperature. Results showed the amount of vapor produced, the temperatures, and the concentrations of liquid in the pot and produced vapor. The simulations were run with the same pressures and temperatures as in the flash model. Results are presented in figures 31 and 32.

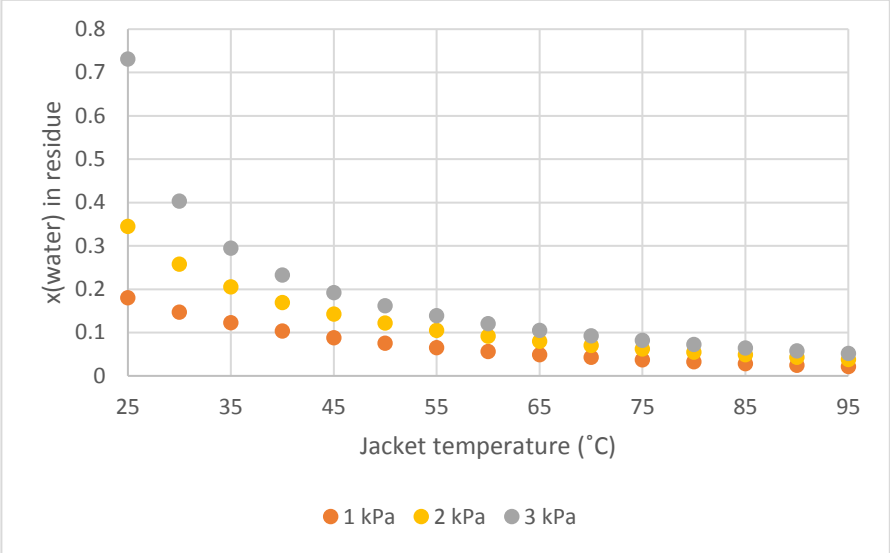

Figure 31. Mass fraction of water in residue. (Batch model)

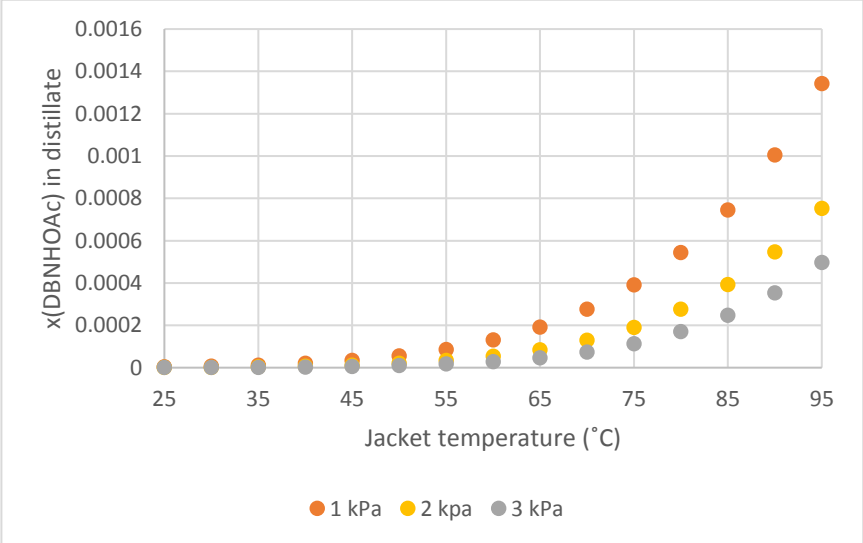

Figure 32. Mass fraction of [DBNH][OAc] in distillate. (Batch model).

6. Comparison of flash and batch models

Flash and batch model performances at different pressures and temperatures were compared. Model comparison is presented in figure 33. In the case of residue composition, both models give identical results. This is because of the fact that the residue in both models is assumed to be at 75 ℃ in equilibrium concentration. Results for distillate composition between the two models are very different. After 35 ℃ the flash model starts to give much higher [DBNH][OAc] compositions compared to the batch model. This is the result of the assumption in flash model that all the vapor and liquid inside the evaporator is at single equilibrium. In batch model, the distillate is a combination of vapor produced at different temperatures and thus it gives much lover [DBNH][OAc] compositions.

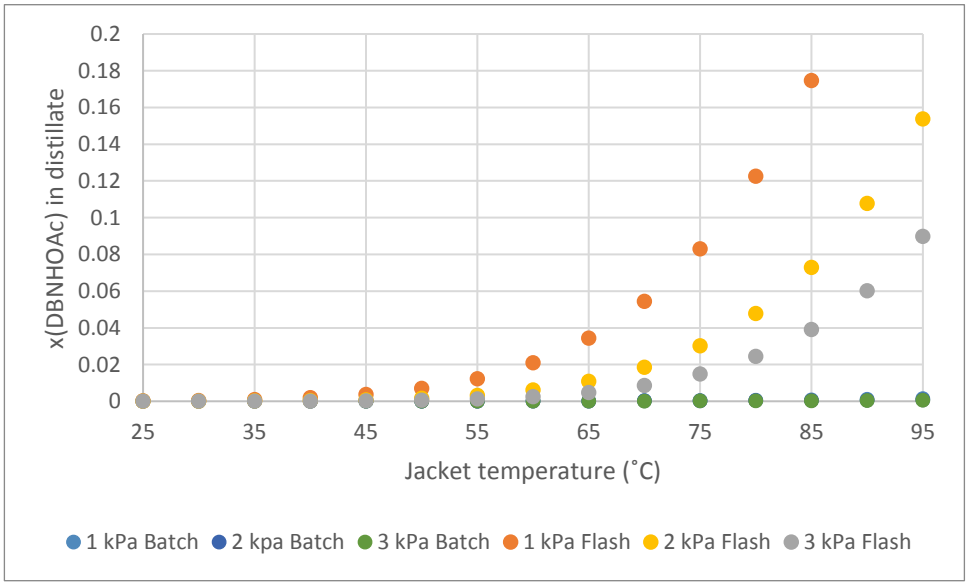

Figure 33. Comparison of [DBNH][OAc] mass fraction in distillate. Results for the batch model are so low compared to the flash model, that they appear by the x axis.

6.1. Comparison with experimental data

To further compare flash and batch models and to validate whether the theory behind flash or batch model is closer to reality, their performances were compared against experimental data. Simulations were run with same feed concentration, evaporator temperature and pressure, as in experiments by Ahmad et al. (2016). In case of batch distillation, the temperature of the produced vapor was also compared to the experimental data. Flash model of course had the same set temperature everywhere.

Simulation results are presented in figures 34-37. Figure 34 shows the water content in residue in simulations matches the experimental results. First couple of experiments show higher deviation between simulation and experimental results. Ahmad et al. (2016) speculated that it could be due to jacket temperature not having completely stabilized. Figure 35 shows that flash model gives too high [DBNH][OAc] content for distillate compared to experimental results. Logarithmic distillate results are shown in figure 36 to better show the difference between experimental and simulation results. Experimental results are in-between the two simulation models, but much closer to batch model.

The temperature of the produced vapor also indicates that the batch model is the better one. Figure 37 shows the vapor temperature for the batch model and the experiments. Temperature of the vapor in flash model is the same as the heating jacket temperature in all the experiments (77-93 °C) so it is not included in the figure 38. Batch model follows the temperature curve of the experiments fairly well. However, it gives lower temperatures compared to experimental results in all 9 cases. This could indicate that some interaction is occurring between vapor and liquid. Other explanation could be the inaccuracy of the VLE-model due to the missing component, hydrolysis product of the [DBNH][OAc].

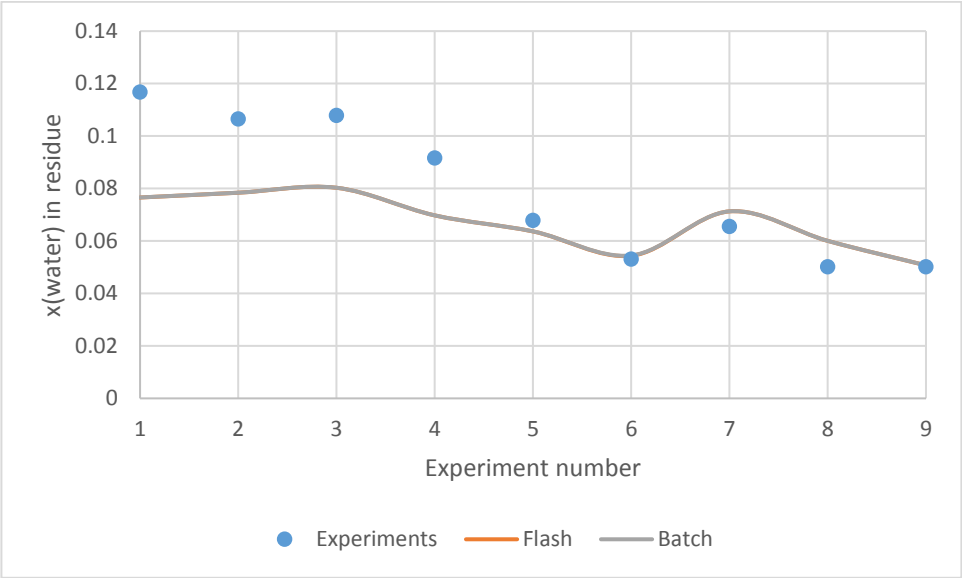

Figure 34. Mass fraction of water in residue. Flash and batch models overlap completely.

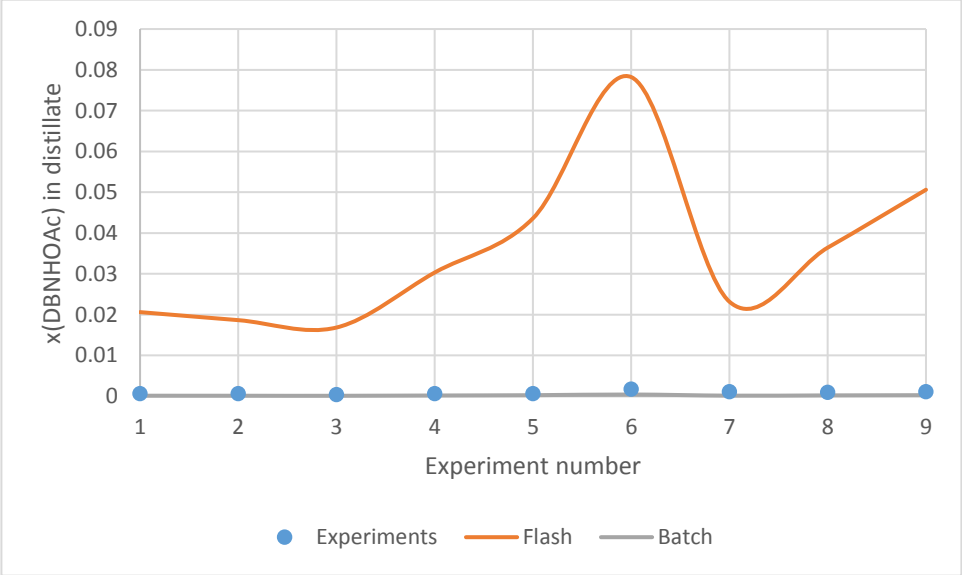

Figure 35. Mass fraction of [DBNH][OAc] in distillate.

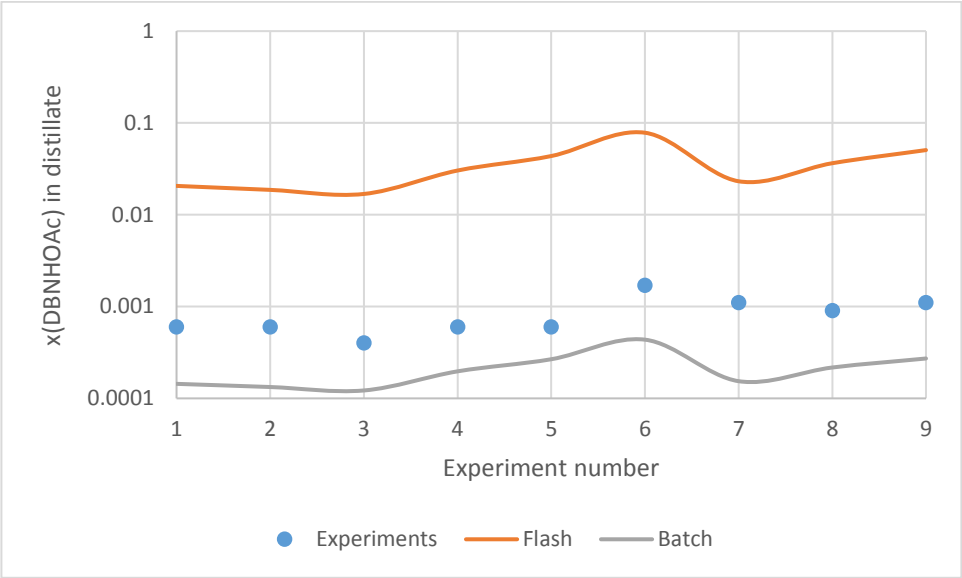

Figure 36. Mass fraction of [DBNH][OAc] in distillate in logarithmic scale.

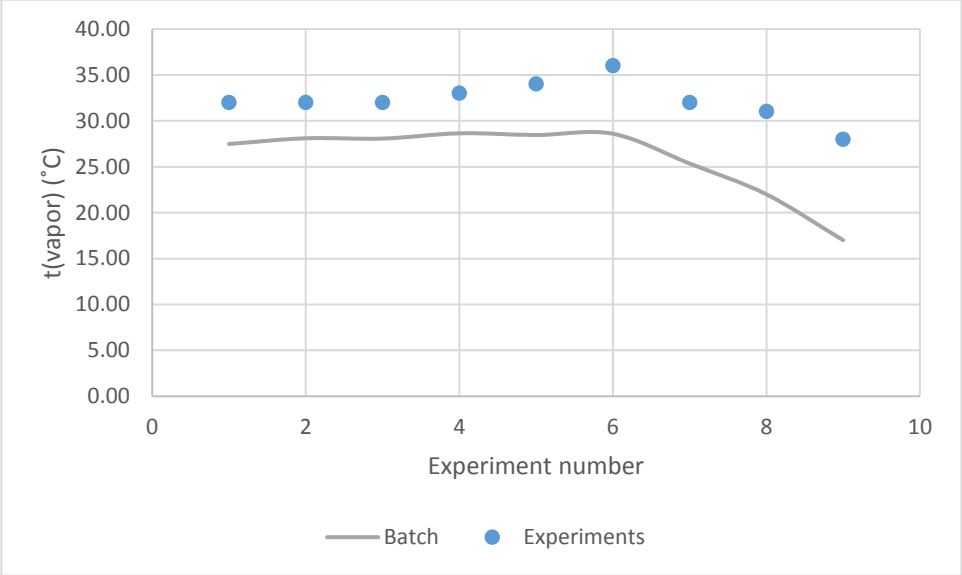

Figure 37. Temperature of the vapor exiting the evaporator.

The experimental results lying between the two models is logical. Flash model assumes total mixing everywhere in the evaporator, batch model assumes no interaction between vapor and

liquid along the evaporator height. Results suggest that in reality, there is some interaction between vapor and liquid but it is not excessive because experimental results are quite far from the flash model results. One thing missing from both models is the hydrolysis product. Including it to the model should give better results but it would require data on its reaction kinetics and physical properties, which are not available.

6.2. Challenges in comparing experimental data with models

When comparing experimental results with models, an anomaly with the feed temperature was discovered. Feed temperature after the feed preheater was measured to be at 78 °C. At the system pressure (varying between 1.6-3.1 kPa) 80-84 w-% of the feed should already have vaporized when entering the evaporator. For feed velocity this would mean absurdly high values. The velocity of the feed in experiment 9 is calculated as an example:

The pressure in the feed pipe is assumed to be the same as in the evaporator, 1.6 kPa. Temperature of the feed entering the evaporator is 78 °C, with feed rate of 4.3 kg/h. Txy-diagram at 1.6 kPa gives a vapor fraction of 0.84 which means vapor flow rate of 3.61 kg/h. Feed pipe diameter is approximately 8 mm / 10 mm. ideal gas law gives a volume flow of 0.102 m^3/h. This would mean flow velocity of 2021 m/s, which would lead to choking condition. This would indicate that there must be a pressure difference between the evaporator and the pipeline before it and that the feed would stay mostly as liquid after the preheater because of the higher pressure. For the whole feed to stay in liquid form at 78 °C, the pressure would have to be 42 kPa according to Pxy-diagram. This pressure difference between the feed pipe and the evaporator would mean adiabatic flash evaporation when feed enters the evaporator and it should be considered in the simulation models if preheater is present.

Preheater also raises the question whether it causes unwanted hydrolysis reaction to occur. Preheating the feed does not seem to have high impact on lowering the needed power in the evaporator due to relatively low boiling point of the feed. It however exposes the feed to unnecessarily high temperatures and may produce hydrolysis product and its irreversible decomposition product APPAc. Same principle applies to residue heater present in experiments by Ahmad et al. (2016). Residue heater was set to 80 °C in all experiments to keep the viscocity

of the residue low. This may also cause production of hydrolysis product and its evaporation, or decomposition into APPAc. It might be beneficial to lower the temperature of the residue heater to avoid unwanted reactions.

Preheater and residue heater are not present in the simulation models and they make it harder to compare simulation results to experiments. It is also currently impossible to include them in the models due to the lack of data on hydrolysis reaction. Experiments should be conducted without the preheater and either without the residue heater or at least with it being set to much lower temperature. The residue has low water concentration so the hydrolysis reaction might be a problem. The results would be more applicable to comparison with models and might show less hydrolysis product formation thus improving [DBNH][OAc] yield and the purity of the produced vapor.

7. Batch model in Aspen Plus

The simulation results suggested that the batch model is more accurate than the flash model and it could be used in the simulation of TFE. Next step was to get batch model applied to steady-state simulation in Aspen Plus.

Transition from flash model in Aspen Plus towards batch model can be achieved by adding multiple flashes in a row. Flashes can be defined by duty or by temperature. To satisfy the theory of no interaction between vapor and liquid, vapor is collected from each flash block to mixer and only liquid flows to the next flash block. This allows steady-state simulation of TFE based on batch theory. Increasing the number of flashes moves the results towards batch results. In theory, infinite amount of flashes should give the same results as the batch model. In practice, multiple flashes with for example 5 °C increase between each flash could be adequate. This batch model consisting of multiple flashes is presented in figure 38.

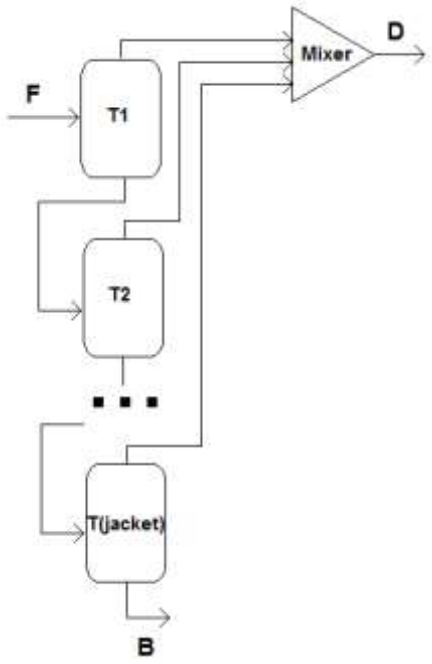

Figure 38. Illustration of batch model as multiple flashes. T1 is boiling point of the liquid at the set evaporator pressure. T(jacket) is the temperature of the heating jacket.

Flash models with different temperature increments were constructed. The aim was to solve an temperature increment that would be satisfactory to produce similar results than the batch model. Feed composition was set to 80 w-% water. Pressure was set to 3 kPa and heating jacket was selected to be at 75 ℃. Temperature of the first flash was set to 25 ℃ (boiling point of the feed at 3 kPa). Models with 2, 5 and 10 ℃ increments were simulated and compared to the single flash model and the results from Batch Modeler. Results are presented in figure 39.

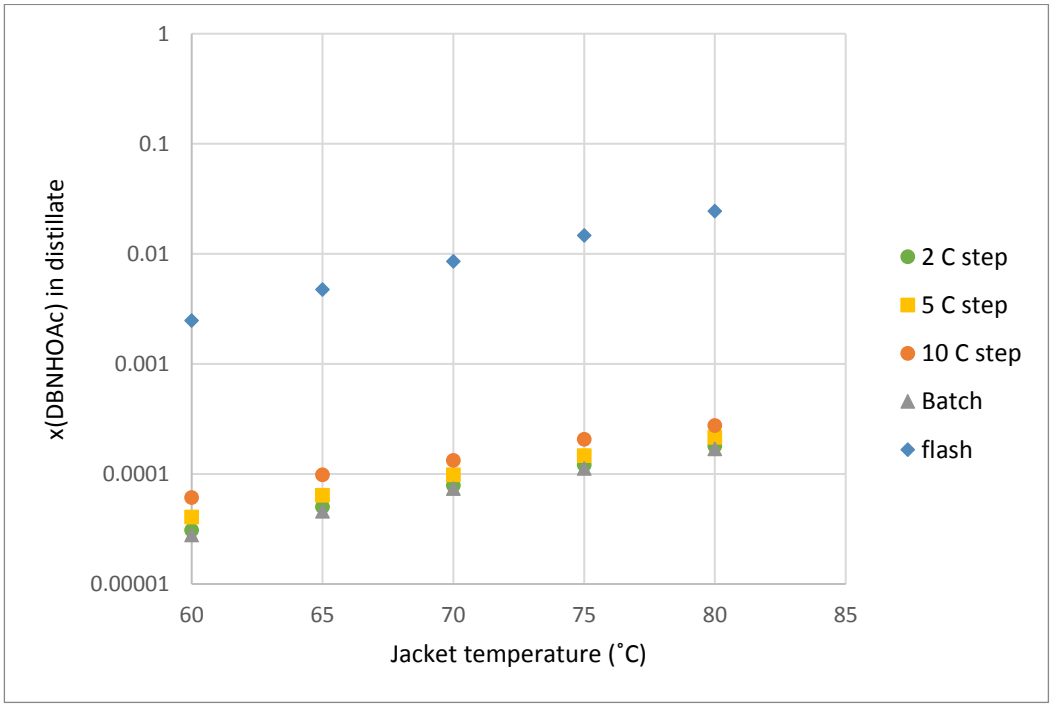

Figure 39. Mass fraction of DBNOAc in distillate. Batch-type multi-flash models vs. batch and flash model.

In the case of total produced vapor, all multi-flash models gave results with less than 1% deviation. Results showed that the models with 5 and 10 ℃ increments between flashes were not accurate enough to provide similar results as the Batch modeler for the [DBNH][OAc] in distillate. The model with 2 ℃ increments gave distillate concentration results very close to the Aspen Batch Modeler. The results for [DBNH][OAc] in distillate were 6.5-10 % higher than the Aspen Batch Modeler results, which is accurate enough considering how small the amount of [DBNH][OAc] in the distillate is. This model could thus be used in the simulation of ATFE in accordance to the batch theory. It should give more accurate results than the single flash model

for residue and distillate flowrates, distillate composition, and required heating power. This developed model is from now on referred as batch-style multiflash model to avoid the confusion with batch model in Aspen Batch modeler.

The idea of fitting the temperature increment to make the results from the model match the experminental results was also considered. It was however deemed useless because if the geometry or some operating parameters of the evaporator or the content of the feed were chanced, the fitting would have to be done again.

8. Case study

A simulation case study was conducted for the batch-style multiflash model. The purpose was to get a better understanding on what is required to achieve a certain water content in the residue with a demonstration plant. Because the experimental results by Ahmad et al. (2016) were in between the two simulation models (chapter 6), flash model was also simulated to give some threshold values to required heating power for example. The use of multiple thin film evaporators with different pressures and temperatures was also considered to help recycling the produced vapor.

Feed was decided to be 80 w-% water. Feed rate was set to be 500 kg/h, approximately 100 times larger than in the bench-scale measurements conducted by Ahmad et al. (2016). Desired water content in the residue was 4 w-%, a maximum acceptable water content mentioned by Parviainen et al. (2015). Due to decomposition of [DBNH][OAc] at high temperatures, a maximum heating jacket temperature was decided to be 85 ℃.

8.1. Single evaporator

A study was first conducted with a single evaporator. Operation pressure of the evaporator was read from VLE-diagram with the temperature limit of 85 ℃ and residue water content of 4 w-%. The required pressure was approximately 1.5 kPa. Feed was set at room temperature 20 ℃ and

atmospheric pressure. Because the boiling point of the feed at 1.5 kPa is 14 °C, an adiabatic flash block was added to both models.

For the single flash model, the flash block was set at 1.5 kPa and 85 °C. For the batch-style multiflash model, temperature of the first flash was set at 14 °C and flashes were added with 2 °C increments up to 85 °C. All flashes were set to 1.5 kPa pressure. Simulation results for both models are presented in table 3.

Table 3. Case study results for flash and batch. IL stands for the ionic liquid [DBNH][OAc]. x = mass fraction.

	residue			**distillate**			**Performance**		
	m(kg/h)	x(water)	x(IL)	m(kg/h)	x(water)	x(IL)	Power(kW)	IL loss (kg/h)	IL yield (%)
flash	54.71	0.0393	0.9607	445.29	0.8935	0.1065	287.12	47.44	52.56
batch	103.87	0.0393	0.9607	396.13	0.9994	0.0006	268.18	0.22	99.78

Even though the residue composition is the same in both models, the distillate results underline the difference between the two models. The batch-style multiflash model gives [DBNH][OAc] a yield of 99.8 % whereas the flash model estimates it to be only 52.6 %. The results for required heating power are much closer to each other. Flash model gives 7 % higher value for required heating power. This suggests that if the heat transfer coefficients are calculated correctly, both models can give reasonably accurate estimates for the required heat exchange surface.

8.2. Multiple-effect evaporator

The case of using multiple-effect evaporator was considered. It could provide a significant decrease in required heating power. It would also bring the effect of separating the produced vapor to multiple streams with different concentrations, which could be beneficial in recycling the water. Utilizing multiple-effect evaporation to this case is challenging because the boiling point of the mixture rises rapidly when the water content gets close to the required 4 %. It can however be partially used because the temperature rise is not significant for the most of the

evaporation. For example in the case of operating at 1.5 kPa, after 90 % of the required heating the temperature has risen from 14 to 22 °C. The rest 10 % of the heating power raises the temperature from 22 to 85 °C. If the first evaporator was at 50 kPa, boiling would start at 82 °C. The vapor from this evaporator could be used as heating power in the next evaporator at 1.5 kPa. Thus, the total required heating power could be significantly reduced. This would also save some cooling power that is required to condensate the produced vapor. A small evaporator with utility heating would be needed as the last step to achieve the desired water content in the residue.

The structure of the double-effect evaporator with additional third evaporator is presented in figure 40. More effects could be implemented if the pressures were selected so that ΔT is enough for heat transfer between the vapor and the liquid. High boiling point at the first evaporator wouldn't necessarily cause hydrolysis reaction because the water content is high at the start.

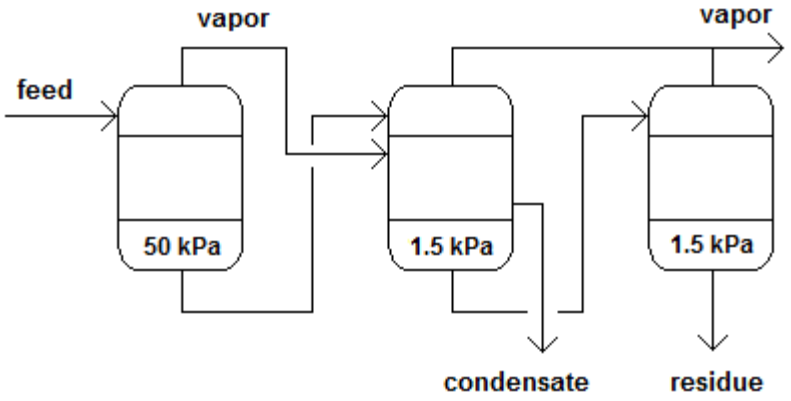

Figure 40. The structure of the double effect evaporator. The first and the third evaporators heated with utility. The second evaporator heated with vapor from the first evaporator.

Example model of double-effect evaporator was constructed and simulated. First evaporator was set to 10 kPa and the second to 1.5 kPa. Third evaporator at 1.5 kPa was needed as well to complete the evaporation. Duty of the first evaporator was set so that all the latent heat of the vapor was usable in the next evaporator. If too much vapor was produced in the first evaporator,

the temperature of the liquid in the next evaporator would rise to the heating vapor temperature and the rest of the vapor could not condensate.

Case study with the same parameters as in chapter 8.1. was conducted. In Aspen Plus the first evaporator was simulated with a single flash because the temperature rise was low. When the first evaporator was heated with 145 kW power, It reached the temperature of 83 °C. The structure of the second evaporator was more rigorous. It started with a flash block at 1.5 kPa with zero duty to simulate adiabatic flashing when the feed enters the second evaporator with lower pressure. The residue from this flash was fed to subsequent pairs of heat exchangers and flashes at 1.5 kPa. Each heat exchanger raised the temperature of the liquid by 2 °C with vapor from the first evaporator. The flashes after each heat exchanger functioned as a phase separation and the residue was fed to the next heat exchanger. After the last heat exchanger the heating vapor was totally condensed and the temperature of the residue was 30 °C. The third evaporator was simulated with 2 °C increment flashes at 1.5 kPa. This Aspen model with three evaporators is presented in figure 41 and the results from the case study are in table 4.

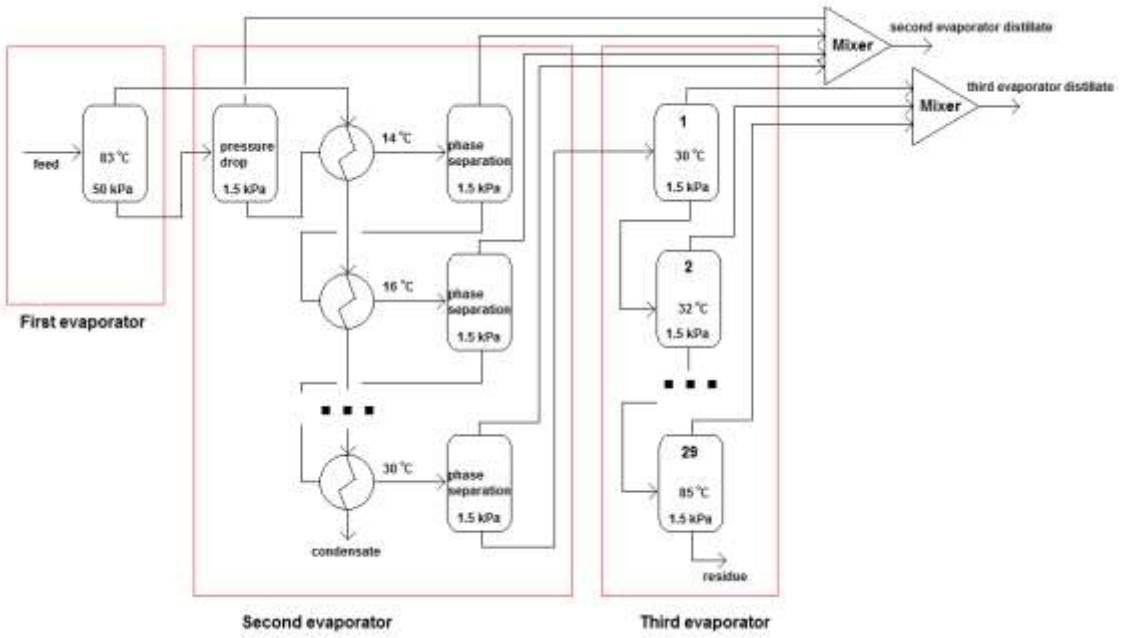

Figure 41. Simplified figure of the double-effect evaporator simulation model in Aspen Plus. Three different evaporators highlighted with red.

Table 2. Case study results for multiple-effect evaporator.

	residue			**distillate**			**performance**		
	m(kg/h)	x(water)	x([DBNH][OAc])	m(kg/h)	x(water)	x([DBNH][OAc])	Power(kW)	IL loss (kg/h)	IL yield (%)
Evaporator 1	323.46	0.6908	0.309	176.54	1	0.0000001	145.40	0.0000	99.999
Evaporator 2	125.52	0.2033	0.797	197.93	0.999994	0.0000056	0	0.0011	99.999
Evaporator 3	103.87	0.0393	0.961	21.66	0.989937	0.0100627	15.83	0.2179	99.782
total							161.23	0.2191	99.781

Results show significant decrease in total required heating power. In the case of single evaporator 268 kW of heating power were required whereas with double-effect evaporator the total heating power is 161 kW. This equals 40 % decrease in required heating power. The distillates from the first two evaporators had DNBHOAc contents of 0.00001 w-% and 0.0006 w-%, whereas the distillate from the third evaporator had much higher 1 w-% [DBNH][OAc] content. There are no values for the required purity of the recycled water in this process but the distillates from the first two processes would almost certainly be pure enough for reuse in washing the produced fibers. The less pure distillate could be reused in the spin bath.

The simulation results support the idea of using multiple-effect evaporation. It would help recycling the evaporated water and reduce required heating power. The case of required heat exchanger surface area is calculated in next chapter to further investigate the usefulness of multiple-effect evaporation.

8.3. Evaporator surface area

The surface areas needed for the different evaporators in the case study were calculated. In the case of single evaporator, heating was selected to be done by 100 °C steam condensing on the evaporator heat exchanger surface. In the multiple-effect evaporator, the first and the third evaporators were also heated by 100 °C steam.

The equations for calculating heat transfer coefficients needed specifications for evaporator geometry. Every evaporator was selected to operate with 4 blades with rotational speed of 400

rpm. The diameter of every evaporator was defined to be five times its height to enable the calculations. Diameter was set as a variable to fit evaporator surface area to the required heat transfer area by iteration.

Equation 3 was used to calculate the outside heat transfer coefficient and equations 9-13 were used to calculate the inside heat transfer coefficient. Evaporator wall was defined to be 5 mm thick steel. Thermal conductivity of the [DBNH][OAc] was not available in the literature, so an approximate value of 0.2 W/mK was used, a common value for conductivity of many different ionic liquids. Thermal conductivity for the binary mixture of water and ionic liquid [DBNH][OAc] was calculated with Fillippov equation:

$$\lambda(mixture) = x_{IL}\lambda_{IL} + x_{water}\lambda_{water} - 0.72x_{IL}x_{water}(\lambda_{water} - \lambda_{IL} \quad (36)$$

The results for evaporator sizes and heat transfer coefficients are presented in table 5.

Table 3. Heat transfer coefficients and evaporator sizes.

single evaporator		**multiple-effect evaporator**		
		evaporator 1	evaporator 2	evaporator 3
d (m)	0.825	0.475	0.49	0.185
h (m)	4.125	2.375	2.45	0.925
h0 (W/m^{2}K)	6435	6516	6892	15051
hp (W/m^{2}K)	881	1955	672	555
U (W/m^{2}K)	622	1002	508	454
A (m^2)	10.7	3.53	3.78	0.54

The results show that the multiple-effect evaporator needed a total of 7.85 m^2 heat transfer area, which is less than the area of 10.7 m^2 in the case of single evaporator. This together with decrease in heating power support the use of multiple-effect evaporation in ionic liquid recycling.

9. Conclusions

Different methods of simulating agitated thin film evaporator were studied in this work. Focus in experimental part was on equilibrium based modeling due to the complexity of rate based modeling and a lack of information on the properties of the ionic liquid. Application of batch distillation theory to thin film evaporation was studied, and it proved to be viable in resembling the evaporation phenomenon inside an agitated thin film evaporator. The batch model was based on the hypothesis that there is no single equilibrium inside the evaporator. The total produced vapor would then be a combination of all the produced vapor with different concentrations at different temperatures. The flash model developed by Ahmad et al. (2016) assumed that the whole evaporator was at an equilibrium at the heating jacket temperature. This assumption works in some cases, but the temperature rise with water/[DBNH][OAc] mixture is significant, which makes flash model with single temperature inaccurate. When compared to the experimental results, the batch model was more accurate than the flash model. It however gave too low [DBNH][OAc] concentration and temperature for the produced vapor. This could be a result of considering the [DBNH][OAc]/water mixture as a binary mixture. In reality, the hydrolysis product of [DBNH][OAc] is also present. As of now, not enough information on the hydrolysis product is available to include it in the model. Other explanation for the deviation of the model results from the experimental results could be unideal mixing of the liquid inside the evaporator. A batch-style multiflash model was developed in Aspen Plus to allow steady-state simulation based on batch theory. Flashes with 2 °C increments were determined to be enough.

A case study was conducted to investigate the use of agitated thin film evaporator in industry-scale process of ionic liquid recycling. This was done by simulating the evaporator in Aspen Plus with batch-style multiflash model. Study concluded that multiple-effect evaporation with agitated thin film evaporators could be a viable option in recycling the ionic liquid and the water.

9.1. Future research

To further develop the batch-style multiflash model in Aspen Plus, evaporation of the hydrolysis product APPHOAc and the hydrolysis reaction should be implemented. Experimental results showed that the distillate had four to ten times more APPHOAc than [DBNH][OAc], hence it is

necessary to include hydrolysis reaction in the model to achieve accurate vapor concentrations in the model. Other way of achieving more accurate results would be rate based modeling, such as done by Rossi et al. (2015), but it would also need more information on [DBNH][OAc] and its reaction product. The focus on further studies should therefore be on the properties and the reactions of APPHOAc, and after that, its implementation to the evaporator model.

References

AHMAD, W., OSTONEN, A., JAKOBSSON, K., UUSI-KYYNY, P., ALOPAEUS, V., HYVÄKKÖ, U. and KING, A.W.T., 2016. Feasibility of thermal separation in recycling of the distillable ionic liquid [DBNH][OAc] in cellulose fiber production. Chemical Engineering Research and Design, 114, pp. 287-298.

AHMED, S.Y. and KAPARTHI, R., 1963. Heat Transfer Studies of Falling Film Heat Exchangers. Indian Journal of Technology, 1, pp. 377-377-381.

BOTT, T.R. and SHEIKH, M.R., 1966. Evaporation at a Scraped Surface. Chemical engineering progress symposium series, 62(64).

BOTT, T.R. and ROMERO, J.J.B., 1963. Heat transfer across a scraped surface. The Canadian Journal of Chemical Engineering, 41(5), pp. 213-219.

CHAWANKUL, N., CHUAPRASERT, S., DOUGLAS, P. and LUEWISUTTHICHAT, W., 2003. Optimisation of an agitated thin film evaporator for concentrating orange juice using AspenPlus. Developments in Chemical Engineering and Mineral Processing, 11(3-4), pp. 309-322.

CHAWANKUL, N., CHUAPRASERT, S., DOUGLAS, P. and LUEWISUTTHICHAT, W., 2001. Simulation of an agitated thin film evaporator for concentrating orange juice using AspenPlusTM. Journal of Food Engineering, 47(4), pp. 247-253.

CHUAPRASERT, S., DOUGLAS, P. and NGUYEN, M., 1999. Data reconciliation of an agitated thin film evaporator using Aspenplus. Journal of Food Engineering, 39(3), pp. 261-267.

DZIAK, J., 2011. Mass and Heat Transfer During Thin-Film Evaporation of Liquid Solutions. Advanced Topics in Mass Transfer.

HÄMMERLE, F.M., 2011. The cellulose gap (the future of cellulose fibers). Lenzinger Berichte, 89, pp. 12-21.

KNUDSEN, J., HOTTEL, H., SAROFIM, A., WANKAT, P. and KNAEBEL, K., 1997. Section 5. Heat and Mass Transfer. Perry's Chemical Engineers' Handbook. 7th edition edn.

LOPEZ-TOLEDO, J., 2006. Heat and Mass Transfer Characteristics of a Wiped Film Evaporator, The University of Texas at Austin.

NUMRICH, R., 1995. Heat transfer in turbulent falling films. Chemical Engineering & Technology, 18(3), pp. 171-177.

OSTONEN, 2016. Experimental and Theoretical Thermodynamic Study of Distillable Ionic Liquid 1,5-Diazabicyclo[4.3.0]non-5-enium Acetate. Industrial & Engineering Chemistry Research, 55(39), pp. 10445-10454.

PARVIAINEN, A., 2015. Sustainability of cellulose dissolution and regeneration in 1,5-diazabicyclo[4.3.0]non-5-enium acetate: A batch simulation of the IONCELL-F process. RSC Advances, 5(85), pp. 69728-69737.

ROSSI, F., CORBETTA, M., GERACI, D., PIROLA, C. and MANENTI, F., 2015. First-principles non-equilibrium dynamic modelling of agitated thin-film evaporators.

SAE TAE, A., 1999. Heat transfer coefficients in an agitated thin film evaporator for concentrating sugar syrup, King Mongkut's University of Technology Thonburi, Bangkok, Thailand.

SCHAAL, F., SCHILLING, K. and HASSE, H., 2008. Separation efficiency of thin-film evaporators: Experiments with water–ethylene glycol and methanol–water and stage-based modeling. Chemical Engineering and Processing: Process Intensification, 47(2), pp. 209-214.

SIEDER, E.N. and TATE, G.E., 1936. Heat transfer and pressure drop of liquids in tubes. Industrial and Engineering Chemistry, 28, pp. 1429-35.

SINGH, R.P. and HELDMAN, D.R., 2009. Introduction to Food Engineering (4th Edition). Elsevier.

VOGEL, H.C. and TODARO, C.M., 2014. Fermentation and Biochemical Engineering Handbook - Principles, Process Design, and Equipment (3rd Edition). Elsevier.

YIH, S. and CHEN, K., 1982. GAS ABSORPTION INTO WAVY AND TURBULENT FALLING LIQUID FILMS IN A WETTED-WALL COLUMN. Chemical Engineering Communications, 17(1-6), pp. 123-136.